Aperture blockage in dual reflector antenna systems : a review

APERTURE BLOCKAGE IN DUAL REFLECTOR ANTENNA SYSTEMS - A REVIEW

by

J. Dijk, J.M. Berends and E.J. Maanders

Technische Hogeschool Eindhoven
Eindhoven Nederland
Afdeling Elektrotechniek

Eindhoven University of Technology
Eindhoven Netherlands
Department of Electrical Engineering

Aperture Blockage in Dual Reflector Antenna Systems - a Review

by

J. Dijk, J.M. Berends and E.J. Maanders

T.H. Report 71-E-23
September 1971

Contents

Summary

This report deals with various aspects of blockage effects on the performance of circularly symmetrical dual reflector antenna systems, where the aperture of the main reflector is partly blocked by a subreflector with four struts. Approximated and exact methods are discussed for calculating the blockage effect on the basis of geometrical optics; a justification of the diffraction effects is given.

Expressions have been found for calculating the influence of the blocked parts on the general directive gain pattern which leads to some interesting conclusions with respect to near sidelobe levels in certain directions. Evaluated examples and general computer programs are given. The same equations may be used as a starting-point for the calculation of the blockage efficiency.

Using power equilibrium equations, the optimum blockage efficiency of shaped cassegrain antenna systems may be calculated.

Finally, the report deals with detailed calculations of the blockage efficiency with respect to several parameters, such as F/D ratio, aperture illumination, dimensions of struts and subreflector and the implantation of the struts on the main reflector. A general computer program is given.

The report also contains an extensive study of the literature on the subject. In some instances refinements and corrections of results and expressions are suggested.

1. *Introduction*

A limitation of most double reflector systems, such as cassegrain antennas, is the blockage of the aperture by the subdish and support legs. Although blockage appears in front-fed paraboloids as well, the consequences are less severe, as the feed is mostly smaller than a subreflector and the support legs much thinner.

Usually, the shadow of the obstacles on the aperture is determined by ray optics . The optical shadows must be weighted by the aperture illumination function to calculate influence on antenna efficiency and sidelobes. However, as Ruze (1) has already pointed out, the radio frequency shadows are wider than optical shadows; therefore, optical shadows form only an approximation. The problem may be solved in first order if we know in what way the field from the subreflector is scattered by the support legs as regards amplitude and phase, as well as the results of this on the currents induced on the main reflector.

Then by using the current distribution or aperture field methods (2, p. 144), the secondary pattern of the reflector may be calculated. However, there is interaction between obstacle and source system, resulting in multiple scattering processes (2, p. 129). This effect may not be neglected here because the support legs extend from the subreflector to the surface of the main reflector. A calculation of the current distribution over the main reflector seems very difficult. A possible approach may be found in the work of Pace (3). Therefore, only approximate methods and experiments will give an answer relating to the influence of the support legs on the radiation pattern. It appears that, in accordance with Trentini (4), Kay (5), and Mei and Van Bladel (6), diffraction may be neglected and that geometrical optical methods can be used very well, providing the thickness of the support legs $2w \geq \lambda$.

It is common knowledge that in a cassegrain system plane and spherical wavefronts are found. It is also known that shadows due to cbstacles depend on the type of wavefront. Shadows in the aperture result in the following effects:

(a) Decrease in antenna gain; this effect can be expressed by the relative blockage coefficient $\frac{\eta_B}{\eta_0}$, where η_0 is the efficiency of the unblocked aperture.

(b) Increase in the sidelobes of the directive gain pattern; different contributions are introduced by the obstacles. Near sidelobes that will change, are investigated in this report. The contribution by the subreflector will be circularly symmetrical, while that by the subreflector support legs is more typically the radiation of a rectangular aperture distribution. There is also wide-angle scattering due to the power which is blocked by the obstacles. No calculations on this phenomenon will be included.

(c) If sidelobes are directed towards sources with high noise temperature, increase in the noise temperature of the antenna will be noticed as energy is spread from the main beam to the sidelobes.

It is the purpose of this report to introduce a method of calculating the influence of blockage on the near sidelobes, as illustrated by several examples, and to discuss several methods of blockage calculation.

2. *Influence of obstructions on the directive gain pattern*

If the aperture of a circularly symmetrical antenna is illuminated uniformly in phase and amplitude, the generalized secondary circularly symmetrical pattern near the main axis (2, p. 194) becomes

$$g(u) = \frac{\pi D^2}{2} \cdot \frac{J_1(u)}{u} \quad , \tag{1}$$

where D is the diameter of the aperture, $J_1(u)$ a Bessel function of the first order and

$$u = \frac{\pi D}{\lambda} \sin \theta \quad . \tag{2}$$

The angle θ constitutes part of a spherical coordinate system (Fig. 1) and for $\theta = 0$ the position of the antenna axis is found. The pattern is independent of ϕ. Silver (2, p. 190-192) assumed that over the exposed area the presence of an obstacle would not alter the amplitude distribution $F(r, \phi')$ which would exist in its absence; therefore the obstacle can be regarded as producing a field equal in amplitude but 180° out of phase with the original field distribution over the area that it covers. In this way zero illumination is obtained over the blocked parts of the aperture. This principle is often called the "zero field concept". Therefore, if the aperture is blocked by a subreflector with a diameter D_s in a cassegrain system, the generalized circularly symmetrical pattern of this subreflector may be represented by

$$g'(u') = \frac{\pi D_s^2}{2} \cdot \frac{J_1(u')}{u'} \quad ,$$

where

$$u' = \frac{\pi D_s}{\lambda} \sin \theta \quad .$$

The modified pattern is then

$$g_t(\theta) = g(u) - g'(u') \quad . \tag{3}$$

These principles will be used to investigate the influence of the blocking obstacles within a cassegrain system on the sidelobes of the secondary pattern.

Recently, Cornbleet (7) has carried out calculations of the radiation pattern of apertures with structural shadows; however, his shadows are not very realistic for cassegrain antennas.

Generally, (2, p. 173) the relative far field directive gain pattern of a rectangular aperture near the main axis may be represented by the scalar equation:

$$g(\theta,\varphi) = \int_A F(x,y)\, e^{jk\sin\theta\,(x\cos\varphi + y\sin\varphi)}\, dx\,dy \tag{4}$$

and that of a circular aperture (2, p. 192) by

$$g(\theta,\varphi) = \int_A F(r,\varphi')\, e^{jkr\sin\theta\cos(\varphi-\varphi')}\, r\,dr\,d\varphi' \ . \tag{5}$$

If we want to know the entire directive gain pattern $g(\theta, \phi)$, we will first calculate $g_o(\theta, \phi)$, being the pattern of the unblocked aperture and subtract from it the contribution $g_1(\theta, \phi)$ of the subreflector and the contributions $g_2(\theta, \phi)$ and $g_3(\theta, \phi)$ being shadows of the supports caused by plane- and spherical waves, respectively. In all cases we shall employ the aperture illumination function (Fig. 2)

$$F(r) = 1 - ar^2 \ , \quad 0 \leqslant r \leqslant \tfrac{1}{2}D \ , \quad 0 \leqslant a \leqslant \left(\frac{2}{D}\right)^2 \ . \tag{6a}$$

The directive gain pattern of the unblocked circular aperture now becomes

$$g_o(\theta,\varphi) = \int_0^{\frac{1}{2}D} r\,dr \int_0^{2\pi} e^{jkr\sin\theta\cos(\varphi-\varphi')}\,d\varphi' - a\int_0^{\frac{1}{2}D} r^3\,dr \int_0^{2\pi} e^{jkr\sin\theta\cos(\varphi-\varphi')}\,d\varphi' \tag{7}$$

or

$$g_o(\theta,\varphi) = 2\pi\left(\tfrac{1}{2}D\right)^2\left\{1 - a\left(\frac{D}{2}\right)^2\right\}\frac{J_1(\frac{1}{2}kD\sin\theta)}{\frac{1}{2}kD\sin\theta} + 4\pi a\left(\frac{D}{2}\right)^4 \frac{J_2(\frac{1}{2}kD\sin\theta)}{(\frac{1}{2}kD\sin\theta)^2} \ , \tag{8}$$

$J_o(x)$, $J_1(x)$ and $J_2(x)$ being Bessel functions of zero, first and second order.

As, in accordance with Abramowitch (8, p. 360),

$$\lim_{x \to 0} \frac{J_1(x)}{x} = 0.5 \tag{9}$$

and

$$\lim_{x \to 0} \frac{J_2(x)}{x^2} = 0.125 \quad ,$$

In the main direction, where $\vartheta = 0$, Eq. 8 becomes

$$g_o(0) = \pi \left(\tfrac{1}{2} D\right)^2 \left\{ 1 - \tfrac{1}{2} a \left(\tfrac{1}{2} D\right)^2 \right\} \quad . \tag{10}$$

This value for $g_o(0)$ will be employed in the following as reference value for the relative pattern of the blocked parts of the aperture.

2.1. *Contribution by the subreflector*

The calculation of the contribution of the subreflector to the radiation pattern is carried out in a similar way as for $g_o(\theta,\phi)$. This contribution is circularly symmetrical, therefore,

$$g_1(\theta) = 2\pi\left(\tfrac{1}{2}D_s\right)^2\left[1 - a\left(\tfrac{1}{2}D_s\right)^2\right]\cdot\frac{J_1\left(\tfrac{1}{2}kD_s\sin\theta\right)}{\tfrac{1}{2}kD_s\sin\theta} + 4\pi a\left(\tfrac{1}{2}D_s\right)^4\cdot\frac{J_2\left(\tfrac{1}{2}kD_s\sin\theta\right)}{\left(\tfrac{1}{2}kD_s\sin\theta\right)^2} \quad (11)$$

On the main axis $\theta = 0$ we find

$$g_1(0) = \pi\left(\tfrac{1}{2}D_s\right)^2\left[1 - \tfrac{1}{2}a\left(\tfrac{1}{2}D_s\right)\right] \quad . \quad (12)$$

Similarly to Eq. 8, Eq. 11 is independent of ϕ.

2.2. *Contribution by the supports due to plane waves*

The shadows in the aperture of the supports caused by plane waves are rectangular (Fig. 3). The form of the shadows will be discussed in more detail in Sec. 5. Here, we will have to use Eq. 4, while Eq. 6 may be rewritten as

$$F(x,y) = 1 - ax^2 - ay^2\,,\quad 0 \leqslant x \leqslant \frac{D}{2}\,,\quad 0 \leqslant y \leqslant \frac{D}{2}\,,\quad 0 \leqslant a \leqslant \left(\frac{2}{D}\right)^2 \quad . \quad (6b)$$

The pattern is then

$$g_2(\theta,\varphi) = \iint\left(1 - ax^2 - ay^2\right)e^{jk\sin\theta(x\cos\varphi + y\sin\varphi)}\,dx\,dy \quad . \quad (13)$$

It is convenient to introduce the new variables $u = k\sin\theta\sin\phi$ and $v = k\sin\theta\cos\phi$.

Eq. 13 then becomes (14)

$$g_2(u,v) = \int e^{jvx}dx\int e^{juy}dy - \int ax^2e^{jux}dx\int e^{juy}dy - \int e^{jvx}dx\int ay^2e^{juy}dy$$

or

$$g_2(u,v) = g_2'(u,v) - g_2''(u,v) - g_2'''(u,v) \quad .$$

After introducing the integration limits we obtain

$$g_1'(u,v) = \int_{-w}^{+w} e^{jvx}dx\left[\int_{-r_o}^{+r_o} e^{juy}dy - \int_{-\frac{1}{2}D_s}^{+\frac{1}{2}D_s} e^{juy}dy\right] + \int_{-w}^{+w} e^{juy}dy\left[\int_{-r_o}^{+r_o} e^{jvx}dx - \int_{-\frac{1}{2}D_s}^{+\frac{1}{2}D_s} e^{jvx}dx\right] \tag{15a}$$

$$g_1''(u,v) = \int_{-w}^{+w} ax^2 e^{jvx}dx\left[\int_{-r_o}^{+r_o} e^{juy}dy - \int_{-\frac{1}{2}D_s}^{+\frac{1}{2}D_s} e^{juy}dy\right] + \int_{-w}^{+w} e^{juy}dy\left[\int_{-r_o}^{+r_o} ax^2 e^{jvx}dx - \int_{-\frac{1}{2}D_s}^{+\frac{1}{2}D_s} ax^2 e^{jvx}dx\right] \tag{15b}$$

$$g_1'''(u,v) = \int_{-w}^{+w} e^{jvx}dx\left[\int_{-r_o}^{+r_o} ay^2 e^{juy}dy - \int_{-\frac{1}{2}D_s}^{+\frac{1}{2}D_s} ay^2 e^{juy}dy\right] + \int_{-w}^{+w} ay^2 e^{juy}dy\left[\int_{-r_o}^{+r_o} e^{jvx}dx - \int_{-\frac{1}{2}D_s}^{+\frac{1}{2}D_s} e^{jvx}dx\right]. \tag{15c}$$

Carrying out the integration leads to

$$g_1'(u,v) = 2w\,\frac{\sin vw}{vw}\left[2r_o\,\frac{\sin ur_o}{ur_o} - D_s\,\frac{D_s \sin u}{D_s u}\right] + 2w\,\frac{\sin uw}{uw}\left[2r_o\,\frac{\sin vr_o}{vr_o} - D_s\,\frac{D_s \sin v}{D_s v}\right], \tag{16a}$$

$$\begin{aligned} g_1''(u,v) = {} & 2wa\,\frac{\sin uw}{uw}\left[2r_o^3\,\frac{\sin vr_o}{vr_o} + \frac{4r_o}{v^2}\cos vr_o - \frac{4}{v^3}\sin vr_o\right] + 2r_o a\,\frac{\sin ur_o}{ur_o}\left[2w^3\,\frac{\sin vw}{vw} + \frac{4w}{v^2}\cos vw - \frac{4}{v^3}\sin vw\right] \\ & + 2wa\,\frac{\sin uw}{uw}\left[\frac{1}{4}D_s^3\,\frac{\sin vD_s}{vD_s} + \frac{2D_s}{v^2}\cos v\cdot\frac{1}{2}D_s - \frac{4}{v^3}\sin v\cdot\frac{1}{2}D_s\right] + aD_s\,\frac{\sin uD_s}{uD_s}\left[2w^3\,\frac{\sin vw}{vw} + \right. \\ & \left. + \frac{4w}{v^2}\cos vw - \frac{4}{v^3}\sin vw\right], \end{aligned} \tag{16b}$$

$$\begin{aligned} g_3'''(u,v) = {} & 2wa\,\frac{\sin vw}{vw}\left[2r_o^3\,\frac{\sin ur_o}{ur_o} + \frac{4r_o}{u^2}\cos ur_o - \frac{4}{u^3}\sin ur_o\right] + 2r_o a\,\frac{\sin vr_o}{vr_o}\left[2w^3\,\frac{\sin uw}{uw} + \frac{4w}{u^2}\cos uw\right. \\ & \left. - aD_s\,\frac{\sin vD_s}{vD_s}\left[2w^3\,\frac{\sin uw}{uw} + \frac{4w}{u^2}\cos uw - \frac{4}{u^3}\sin uw\right] + 2wa\,\frac{\sin vw}{vw}\left[\frac{1}{4}D_s^3\,\frac{\sin uD_s}{uD_s} + \frac{2D_s}{u}\cos u\cdot D_s - \frac{4}{u^3}\sin u\,\frac{1}{2}D_s\right]\right]. \end{aligned}$$

If uniform aperture distribution is used (a = 0), only Eqs. 15a and 16a are left over. In the direction of the main lobe, where $\theta = 0$, we find

$$g_1(0,0) = 8w\left(r_o - \frac{1}{2}D_s\right) - 8aw\left[\frac{1}{3}r_o^3 - \frac{1}{3}\left(\frac{1}{2}D_s\right)^3\right] - 8aw^3\left(\frac{1}{3}r_o - \frac{1}{6}D_s\right). \tag{17}$$

2.3. *Contribution by the supports due to spherical waves*

As observed before (9, 10), the shadows from the supports due to spherical waves are very similar to trapezoids. We will introduce this approximation as it reduces calculation work and makes possible a convenient solution of the integrals. From Fig. 4 it is found that for the trapezoid lying in the area indicated by $r_o < x < \frac{1}{2}D$, y as a function of x is given by

$$y(x>0) = \beta x + w - \beta r_o = \beta x + \gamma$$

with $\beta = \dfrac{w\left(\frac{D}{D_s} - 1\right)}{\frac{1}{2}D - r_o}$ and $\gamma = w - \beta r_o$.

For $-\frac{1}{2}D \leqslant x \leqslant -r_o$ we find $y(x<0) = -\beta x + \gamma$.

For the trapezoid parts along the y axis, x is written as a function of y:

$$x(y>0) = \beta y + \gamma \quad , \quad x(y<0) = -\beta y + \gamma \ .$$

If $u = k\sin\theta\sin\phi$ and $v = k\sin\theta\cos\phi$, the complete expression for the contribution of spherical waves then is

$$\begin{aligned} g_3(u,v) = &\int_{-y(x>0)}^{+y(x>0)} \int_{r_o}^{\frac{1}{2}D} (1 - ax^2 - ay^2)\, e^{jvx} e^{juy}\, dx\,dy \\ &+ \int_{-y(x<0)}^{+y(x<0)} \int_{-\frac{1}{2}D}^{-r_o} (1 - ax^2 - ay^2)\, e^{jvx} e^{juy}\, dx\,dy \\ &+ \int_{-x(y>0)}^{+x(y>0)} \int_{r_o}^{\frac{1}{2}D} (1 - ax^2 - ay^2)\, e^{jvx} e^{juy}\, dx\,dy \\ &+ \int_{-x(y<0)}^{+x(y<0)} \int_{-\frac{1}{2}D}^{-r_o} (1 - ax^2 - ay^2)\, e^{jvx} e^{juy}\, dx\,dy \ , \end{aligned} \tag{18}$$

Carrying out the integration leads to

$$g_3(u,v) = \frac{2}{u.q}\left[1 - a\left\{r_o^2 + (\beta r_o+\gamma)^2 - \frac{2+2\beta^2}{q^2} - \frac{2\beta}{u.q} - \frac{2}{u^2}\right\}\right]\cos(\gamma u + r_o q)$$

$$- \frac{2}{u.p}\left[1 - a\left\{r_o^2 + (\beta r_o+\gamma)^2 - \frac{2+2\beta^2}{p^2} + \frac{2\beta}{u.p} - \frac{2}{u^2}\right\}\right]\cos(\gamma u - r_o p)$$

$$- \frac{2}{u.q}\left[1 - a\left\{\left(\frac{D}{2}\right)^2 + \left(\beta\frac{D}{2}+\gamma\right)^2 - \frac{2+2\beta^2}{q^2} - \frac{2\beta}{u.q} - \frac{2}{u^2}\right\}\right]\cos\left(\gamma u + \frac{D}{2}q\right)$$

$$+ \frac{2}{u.p}\left[1 - a\left\{\left(\frac{D}{2}\right)^2 + \left(\beta\frac{D}{2}+\gamma\right)^2 - \frac{2+2\beta^2}{p^2} + \frac{2\beta}{u.p} - \frac{2}{u^2}\right\}\right]\cos\left(\gamma u - \frac{D}{2}p\right) \qquad (19a)$$

$$+ \frac{4a}{up}\left[r_o\left(\frac{1+\beta^2}{q} + \frac{\beta}{u}\right) + \frac{\beta\gamma}{q} + \frac{\gamma}{u}\right]\sin(\gamma u + r_o q)$$

$$+ \frac{4a}{up}\left[r_o\left(\frac{1+\beta^2}{p} - \frac{\beta}{u}\right) + \frac{\beta\gamma}{p} - \frac{\gamma}{u}\right]\sin(\gamma u - r_o p)$$

$$- \frac{4a}{uq}\left[\frac{D}{2}\left(\frac{1+\beta^2}{q} + \frac{\beta}{u}\right) + \frac{\beta\gamma}{q} + \frac{\gamma}{u}\right]\sin\left(\gamma u + \frac{D}{2}q\right)$$

$$- \frac{4a}{up}\left[\frac{D}{2}\left(\frac{1+\beta^2}{p} - \frac{\beta}{u}\right) + \frac{\beta\gamma}{p} - \frac{\gamma}{u}\right]\sin\left(\gamma u - \frac{D}{2}q\right) \qquad (19b)$$

$$+ \frac{2}{vt}\left[1 - a\left\{r_o^2 + (\beta r_o+\gamma)^2 - \frac{2+2\beta^2}{t^2} - \frac{2\beta}{vt} - \frac{2}{v^2}\right\}\right]\cos(\gamma v + r_o t)$$

$$- \frac{2}{vs}\left[1 - a\left\{r_o^2 + (\beta r_o+\gamma)^2 - \frac{2+2\beta^2}{s^2} + \frac{2\beta}{vs} - \frac{2}{v^2}\right\}\right]\cos(\gamma v - r_o s)$$

$$- \frac{2}{vt}\left[1 - a\left\{\left(\frac{D}{2}\right)^2 + \left(\beta\frac{D}{2}+\gamma\right)^2 - \frac{2+2\beta^2}{t^2} - \frac{2\beta}{vt} - \frac{2}{v^2}\right\}\right]\cos\left(\gamma v + \frac{D}{2}t\right)$$

$$+ \frac{2}{vs}\left[1 - a\left\{\left(\frac{D}{2}\right)^2 + \left(\beta\frac{D}{2}+\gamma\right) - \frac{2+2\beta^2}{s^2} + \frac{2\beta}{vs} - \frac{2}{v^2}\right\}\right]\cos\left(\gamma v - \frac{D}{2}s\right) \qquad (19c)$$

$$+\frac{4a}{vt}\left[r_0\left(\frac{1+\beta^2}{t}+\frac{\beta}{v}\right)+\frac{\beta\gamma}{t}+\frac{\gamma}{v}\right]\sin(\gamma v+r_0 t)$$

$$+\frac{4a}{vs}\left[r_0\left(\frac{1+\beta^2}{s}-\frac{\beta}{v}\right)+\frac{\beta\gamma}{s}-\frac{\gamma}{v}\right]\sin(\gamma v-r_0 s)$$

$$-\frac{4a}{vt}\left[\frac{D}{2}\left(\frac{1+\beta^2}{t}+\frac{\beta}{v}\right)+\frac{\beta\gamma}{t}+\frac{\gamma}{v}\right]\sin\left(\gamma v+\frac{D}{2}t\right) \qquad (19d)$$

$$-\frac{4a}{vs}\left[\frac{D}{2}\left(\frac{1+\beta^2}{s}-\frac{\beta}{v}\right)+\frac{\beta\gamma}{s}-\frac{\gamma}{v}\right]\sin\left(\gamma v-\frac{D}{2}s\right) \quad ,$$

where $v-u\beta=p$, $u-v\beta=s$, $v+u\beta=q$ and $u+v\beta=t$.

For $\theta = 0$ we find in the main direction

$$g_3(0,0)=8\gamma\left(1-\tfrac{1}{3}a\gamma^2\right)\left(\tfrac{1}{2}D-r_0\right)+4\beta\left(1-a\gamma^2\right)\left\{\left(\tfrac{1}{2}D\right)^2-r_0^2\right\}$$
$$-\frac{8}{3}a\gamma\left(\beta^2+1\right)\left\{\left(\tfrac{1}{2}D\right)^3-r_0^3\right\}-2a\beta\left(\tfrac{1}{3}\beta^2+1\right)\left\{\left(\tfrac{1}{2}D\right)^4-r_0^4\right\} \quad . \qquad (20)$$

2.4. *Total directive gain pattern* $g_t(\theta,\phi)$

The expressions found above enable us to find the total pattern $g_t(\theta,\phi)$ in the Fraunhofer zone in accordance with the "zero field concept". As has been explained before (11), the results are only valid for the main lobe and the near sidelobes. We will find that

$$g_t(\theta,\varphi)=g_0(\theta,\varphi)-g_1(\theta)-g_2(u,v)-g_3(u,v) \quad , \qquad (21)$$

where $g_0(\theta,\phi)$ represents the pattern of an unblocked aperture given by Eq. 8; $g_1(\theta)$ the contribution to the pattern by the subreflector (Eq. 11); $g_2(u,v)$ the contribution to the pattern due to plane wave shadows (Eq. 16); and $g_3(u,v)$ the contribution to the pattern due to spherical wave shadows (Eq.19). Further,

$u = k\sin\theta\sin\varphi$ and $v = k\sin\theta\cos\varphi$, k being $\frac{2\pi}{\lambda}$.

In this way the radiation pattern of a cassegrain antenna near the main lobe may be found as a function of several variables, such as the edge illumination of the main reflector, the thickness of the subreflector supports, the ratio D_s/D, the F/D ratio, and the strut implantation.

Some examples, particularly for satellite communication ground station antennas are shown in Figs. 11 and 12. In these cases uniform illumination is used ($a = 0$), $2w = 2\lambda$, and $\phi = 0$ or $\phi = 45^{o}$. The position of the first, second, and third side lobes and their intensity with respect to that of the main lobe are shown. Figs. 11a and 12a show main and side lobes of the blocked and unblocked aperture in dB, and Figs. 11b and 12b the relative pattern of the contributors to the blockage.

The main part of the results for other edge illuminations or different widths of the supports is shown in two tables, one for $\phi = 0^{o}$ and one for $\phi = 45^{o}$ (Tables 1 and 2). More detailed information with regard to the plots may be obtained using the computer programs, described in Appendix B.

Table 1 $D = 333\lambda$; $D/D_s = 10$; $r_o = \frac{1}{3} D$; $\phi = 0$;

$a_1 = 0$ (uniform illumination)

		Main lobe		1st side lobe		2nd side lobe		3rd side lobe	
	2w	θ in 0^{o}	dB	θ in 0^{o}	dB	θ in 0^{o}	dB	θ in 0^{o}	dB
G_o		.000	0.00	.283	-17.6	.465	-23.8	.642	-28.0
G_t	1λ	.000	-0.26	.286	-16.5	.469	-27.0	.647	-25.2
G_t	2λ	.000	-0.41	.288	-16.1	.473	-29.2	.652	-24.2
G_t	3λ	.000	-0.59	.290	-15.7	.477	-31.9	.657	-23.4
G_t	4λ	.000	-0.76	.293	-15.3	.482	-35.3	.662	-22.8
G_t	5λ	.000	-0.94	.296	-14.9	.487	-39.8	.667	-22.3

a_1 = 0.7 (edge illumination -10dB)

		Main lobe		1st side lobe		2nd side lobe		3rd side lobe	
	2w	θ in 0°	dB	θ in 0°	dB	θ in 0°	dB	θ in 0°	dB
G_o	-	.000	0.00	.314	-22.4	.489	-29.6	.662	-34.1
G_t	1λ	.000	-0.28	.316	-20.2	.494	-38.6	.666	-28.3
G_t	5λ	.000	-0.86	.324	-17.8	-	-	.690	-24.4

a_1 = 0.9 (edge illumination -20dB)

G_o	-	.000	0.00	.336	-24.3	.515	-32.8	.688	-38.3
G_t	1λ	.000	-0.29	.338	-21.3	.521	-64.8	.693	-29.7
G_t	5λ	.000	-0.82	.345	-18.8	-	-	.720	-25.3

Table 2 D = 333λ; D/D_s = 10; $r_o = \frac{1}{3} D$; $\phi = 45^o$

a_1 = 0 (uniform illumination)

		Main lobe		1st side lobe		2nd side lobe		3rd side lobe	
		θ in 0°	dB	θ in 0°	dB	θ in 0°	dB	θ in 0°	dB
G_o	-	.000	0.00	.283	-17.6	.465	-23.8	.642	-28.0
G_t	1λ	.000	-0.25	.283	-17.8	.460	-25.8	.635	-25.4
G_t	2λ	.000	-0.42	.283	-18.7	.456	-26.5	.629	-24.5
G_t	3λ	.000	-0.59	.283	-19.7	.449	-27.0	.624	-23.7
G_t	4λ	.000	-0.76	.283	-20.8	.443	-27.3	.620	-23.0
G_t	5λ	.000	-0.94	.283	-22.0	.438	-27.4	.616	-22.3

a_1 = 0.7 (edge illumination -10dB)

G_o	-	.000	0.00	.314	-22.4	.489	-29.6	.662	-34.1
G_t	1λ	.000	-0.28	.314	-21.7	.484	-35.7	.651	-29.1
G_t	5λ	.000	-0.86	.317	-26.0	.460	-39.7	.631	-26.5

a_1 = 0.9 (edge illumination -20dB)

G_o	-	.000	0.00	.336	-24.3	.515	-32.8	.688	-38.3
G_t	1λ	.000	-0.29	.337	-22.8	.511	-46.9	.676	-31.1
G_t	5λ	.000	-0.82	.340	-26.3	-	-	.651	-29.3

2.5. *Results and conclusions*

Studying Fig. 11b in the $\phi = 0$ plane, it appears that $g_1(\phi)$ varies only little within the region under discussion. Comparison of $g_1(\theta)$ with $g_o(\theta)$ shows that these two patterns are equivalent in the case of uniform illumination n; however, the θ scale of $g_1(\theta)$ has been extended by a factor nearly 10. This is due to the fact that the relation $D/D_s = 10$ has been used and that $\sin\theta \approx \theta$.

The contributions of $g_2(u,v)$ and $g_3(u,v)$ in the $\phi = 0$ plane are positive within the entire region under discussion. This fact is explained by considering that the contributions of an array of two supports located in the $\phi = 90^o$ plane to the final pattern are nearly constant, and that those in the $\phi = 0^o$ plane are alternating but not in such a way that the amplitude of g_2 plus g_3 becomes negative.
The situation in the $\phi = 45^o$ plane differs entirely from that in the $\phi = 0^o$ plane (Fig. 12) because now the amplitudes of the patterns g_2 and g_3 are alternatively positive and negative. This is due to the fact that the supports are located symmetrically around the $\phi = 45^o$ plane and the main terms of Eqs. 16 and 19 all have the same sign and all give similar contributions. This phenomenon is noticed in all investigations independent of the edge illumination and of the width of the struts.
If we study the results from tables 1 and 2 it appears that the peak intensity of the main lobe of a blocked aperture is somewhat less than that of an unblocked aperture. In the case of $\phi = 0$, the intensity of the first side lobe increases with increasing width of the supports. This is noticed for all edge illuminations. However, if $\phi = 45^o$ the opposite occurs and the peak intensity of the first side lobes decreases with increasing adge illumination; only for small values of w e.g. $2w = \lambda$ little or no increase or decrease is noticed. Similar phenomena have been observed earlier in experiments (12,13).
This effect may be used with advantage for the location of the supports of antennas for satellite communication ground stations to obtain lower side lobes in certain directions, in the case of terrestrial link interference.
If the width of the supports $2w < \lambda$, the above method is no longer valid due to diffraction effects.

3. *Power balance of the blocked aperture*

If there is no spillover around the edge of the subreflector and the total power P_T radiated by the feedhorn is intercepted by the subreflector, the power reradiated by the aperture is found by subtracting the power P_B blocked by the obstacles from the total power P_T.

Let the coordinates of a point in the aperture be (ξ, η) and the electrical field over the aperture $F(\xi, \eta)$. The total power radiated by the non-blocked aperture is, according to Silver (2, p.177),

$$P_T = \frac{1}{2}\left(\frac{\varepsilon}{\mu}\right)^{\frac{1}{2}} \int_A \left|F(\xi,\eta)\right|^2 (\bar{i}_z \cdot \bar{s})\, d\xi\, d\eta \quad . \tag{22}$$

In this equation $\bar{s}$ is the a vector along a ray (2, p.170) and $\bar{i}_z$ the unit vector perpendicular to the aperture along the z-axis. For $\theta = 0$, in the case of a paraboloid reflector, the rays are parallel to the z-axis so that $(\bar{i}_z \cdot \bar{s}) = 1$.

If the aperture is blocked by a number of obstacles (Fig. 5a and 5b) totalised by $B = \sum_{n=1}^{n=m} B_n$, the blocked power becomes

$$P_B = \frac{1}{2}\left(\frac{\varepsilon}{\mu}\right)^{\frac{1}{2}} \int_B \left|F(\xi,\eta)\right|^2 d\xi\, d\eta \quad . \tag{23}$$

This part of the total power P_T is radiated by the primary feed but it cannot be reradiated by the blocked aperture in the normal way, because it will be scattered in all directions by the feed support, feed cone, subdish and main dish. The directive gain function of a lossless antenna is expressed by $G(\theta,\phi)$, where θ and ϕ are spherical coordinates illustrated in Fig. 1. This function must also satisfy the relation

$$\int_{4\pi} G(\theta,\varphi)\, d\Omega = 4\pi \quad , \tag{24}$$

$d\Omega$ being the element of solid angle.

If $P(\theta,\phi)$ is the power radiated by the antenna per unit solid angle in the direction θ,ϕ, and P_T the total power radiated, the gain is defined as

$$G(\theta,\varphi) = \frac{4\pi P(\theta,\varphi)}{P_T} \quad . \tag{25}$$

The power reradiated by the aperture less the blocked areas will now be equal not to Eq. (22) but to

$$P_T - P_B = \frac{1}{2}\left(\frac{\varepsilon}{\mu}\right)^{\frac{1}{2}} \int_{A-B} |F(\xi,\eta)|^2 \, d\xi \, d\eta \quad . \tag{26}$$

This equation shows that the surface integral extends over the aperture surface A less the blocked surfaces B. A new gain function $\zeta'(\theta,\varphi) = 4\pi \frac{P'(\theta,\varphi)}{P_T}$ will now be formed depending on the power $P'(\theta,\phi)$ radiated per unit solid angle, whereas

$$\int_{4\pi} P'(\theta,\varphi) \, d\Omega = P_T - P_B \quad . \tag{27}$$

This new gain function, in which the blocked power is not transported correctly to the aperture, is now determined by

$$\text{or} \quad \int_{4\pi} \zeta'(\theta,\varphi) \, d\Omega \neq 4\pi$$

$$\text{or} \quad \int_{4\pi} \zeta'(\theta,\varphi) \, d\Omega = 4\pi \left[1 - \frac{P_B}{P_T}\right]$$

$$\int_{4\pi} \zeta'(\theta,\varphi) \, d\Omega = 4\pi - \frac{2\pi}{P_T}\left(\frac{\varepsilon}{\mu}\right)^{\frac{1}{2}} \int_B |F(\xi,\eta)|^2 \, d\xi \, d\eta \quad . \tag{28}$$

The power P_B is scattered by the subreflector, main reflectors support legs, feed and feedcone and adds new contributions to the antenna pattern $G'(\theta,\phi)$, so that the power balance is restored. This scattered power radiates in various directions which are difficult to predict. The antenna pattern $G'(\theta,\phi)$ with supplementary contributions from the scattered power P_B may increase the noise temperature of the antenna if these contributions are directed towards noise sources at high temperatures. Apparently, the blocked power increases the sidelobe level and the antenna noise temperature as well. Therefore, the total influence of blocking parts on the aperture results in a double effect, viz.,

(1) a decrease in the blockage efficiency η_B/η_0 and an increase in the sidelobe level, with the possibility of higher antenna aperture, as in classical systems the blocked power P_B is not available for reradiation by the non-blocked parts of the aperture; in this report this effect is studied in detail for the region near the main axis of the antenna.

(2) an increase in the side lobe level, due to the blocked power P_B being scattered, and, hence higher noise temperatures. This effect is difficult to calculate and will not be discussed in this report.

4. *Blockage efficiency in general*

4.1. *Basic expressions*

Let A be a non-blocked aperture and the coordinates of an aperture field (ξ,η). Let the aperture field be $F(\xi,\eta)$. If the phase is constant over the aperture, the directivity obtained for $\theta = 0$ is, according to Silver (2,p.177),

$$G_A = \frac{4\pi}{\lambda^2} \frac{\left| \int_A F(\xi,\eta)\, d\xi\, d\eta \right|^2}{\int_A |F(\xi,\eta)|^2 d\xi\, d\eta}, \tag{29}$$

where $d\xi d\eta$ represents an elementary area of the aperture.
From Eq. 4 it follows that

$$\int_A F(\xi,\eta)\, d\xi\, d\eta = g_A(0,0) \quad . \tag{30}$$

If the aperture illumination is uniform in amplitude and phase, $F(\xi,\eta)$ will be a constant. In that case, we find from Eqs. 29 and 30 that

$$G_{max} = \frac{4\pi A}{\lambda^2} \tag{31}$$

and $g_A(0,0) = A$, being the geometrical surface of the aperture.
We may also introduce the effective aperture A_{eff} by

$$A_{eff} = \frac{\left| \int_A F(\xi,\eta)\, d\xi\, d\eta \right|^2}{\int_A |F(\xi,\eta)|^2 d\xi\, d\eta} \quad . \tag{32}$$

Substituting Eqs. 30 and 32 in Eq.29 and realizing that the total power equals

$$P_T = \frac{1}{2} \sqrt{\frac{\varepsilon}{\mu}} \int_A |F(\xi,\eta)|^2 d\xi\, d\eta \,, \tag{33}$$

we obtain

$$A_{eff} = \frac{|g_A(0,0)|^2}{P_T} \cdot \frac{1}{2} \sqrt{\frac{\varepsilon}{\mu}} \quad . \tag{34}$$

The illumination efficiency η_o of this non-blocked aperture will now be defined by the relation

$$\eta_o = \frac{1}{A} \frac{\left| \int_A F(\xi,\eta)\, d\xi\, d\eta \right|^2}{\int_A |F(\xi,\eta)|^2 d\xi\, d\eta} = \frac{A_{eff}}{A} \quad . \tag{35}$$

The integral $\int_A |F(\xi,\eta)|^2 d\xi d\eta$ is a measure of the power radiated by the primary feed and intercepted by the main reflector if no spillover is present. The integral $g_A(0,0) = \int_A F(\xi,\eta) d\xi\, d\eta$ is proportional to the field intensity on the main axis.

For circularly symmetrical aperture field distributions, $d\xi.d\eta$ of Eq.35 may be replaced by $2\pi r dr$, where r is the radial distance of the elementary area from the center of the aperture. Eq. 29 then becomes

$$G_A = \frac{8\pi^2}{\lambda^2} \frac{\left| \int_0^{\frac{1}{2}D} f(r)\, r\, dr \right|^2}{\int_0^{\frac{1}{2}D} |f(r)|^2 r\, dr} \tag{36}$$

and Eq. 35

$$\eta_o = \frac{2\pi}{A} \frac{\left| \int_0^{\frac{1}{2}D} f(r)\, r\, dr \right|^2}{\int_0^{\frac{1}{2}D} |f(r)|^2 r\, dr} \quad , \tag{37}$$

if D is the diameter of this circular aperture.

Let the aperture be blocked by a number of obstacles B_1, B_2, B_3, -------B_n (Fig. 5) with

$$g_n(0,0) = \int_{B_n} F(\xi,\eta)\, d\xi\, d\eta \quad , \tag{38a}$$

and

$$B_n(0,0) = \frac{|g_n(0,0)|^2}{P_T} \cdot \frac{1}{2} \sqrt{\frac{\varepsilon}{\mu}} \quad , \tag{38b}$$

where $B_n(0,0)$ is the effective aperture surface of the blocked parts, and let G_T be the gain of the aperture A containing the blocking obstacles B. The efficiency η_B of the blocked aperture is now found to be

$$\eta_B = \frac{G_T}{G_{max}}$$

or

$$\eta_B = \frac{1}{A} \frac{\left| \int_{A-B} F(\xi,\eta)\, d\xi\, d\eta \right|^2}{\int_A |F(\xi,\eta)|^2 d\xi\, d\eta} \quad , \tag{39}$$

where

$$B = \sum_{n=1}^{n=m} B_n \quad .$$

Comparing the efficiency of the blocked and non-blocked apertures, we obtain the relative efficiency

$$\frac{\eta_B}{\eta_0} = \left| \frac{\int_{A-B} F(\xi,\eta)\, d\xi\, d\eta}{\int_A F(\xi,\eta)\, d\xi\, d\eta} \right|^2 = \left| \frac{g_{A-B}(0,0)}{g_A(0,0)} \right|^2 . \tag{40}$$

The integral $\int_{A-B} F(\xi,\eta)\, d\xi\, d\eta$ is equivalent to

$$\int_{A-B} F(\xi,\eta)\, d\xi\, d\eta - \int_B F(\xi,\eta)\, d\xi\, d\eta = g_A(0,0) - g_B(0,0)$$

so that

$$\frac{\eta_B}{\eta_0} = \left| 1 - \frac{\int_B F(\xi,\eta)\, d\xi\, d\eta}{\int_A F(\xi,\eta)\, d\xi\, d\eta} \right|^2 = \left| 1 - \frac{g_B(0,0)}{g_A(0,0)} \right|^2 . \tag{41}$$

In the same way the blockage efficiency for a circularly symmetrical aperture with circularly symmetrical illumination may be expressed by

$$\frac{\eta_B}{\eta_0} = \left| 1 - \frac{\int_B F(r)\, r\, dr}{\int_A F(r)\, r\, dr} \right|^2 . \tag{42}$$

In the case of uniform illumination, $F(\xi,\eta)$ is a constant. Therefore,

$$\frac{\eta_B}{\eta_0} = \left| 1 - \frac{B}{A} \right|^2 , \tag{43}$$

A and B being geometrical surfaces.

Calculations with tapered illumination are presented in Sec. 5.3.
In the following sections it will be proved that the blockage efficiency $\frac{\eta_B}{\eta_0}$ can be further increased to a maximum of

$$\frac{\eta_B}{\eta_0} = \left| 1 - \frac{\Sigma B_{plane}}{A} \right| \tag{44}$$

if the aperture is illuminated uniformly, and ΣB plane represents the parts blocked by plane waves.

4.2. *Optimizing the blockage efficiency*

In sec. 3 it was already found that part of the total power P_T radiated by the feed will not be reradiated by the blocked aperture in the proper way, as it does not reach the aperture in the correct direction and phase. The result is that this power is scattered in all directions, decreasing antenna gain and blockage efficiency.

If the antenna is used for receiving purposes it is easely shown that power of the incoming waves is intercepted by the obstacles. This intercepted power is always wasted and can never be supplied to the feed of the antenna system correctly as it does not have the correct phase or direction of propagation. In the remaining part of this section it will be proved that the blockage efficiency may be increased considerably.

Let $F(\xi,\eta)$ be the field over a non-blocked aperture and $F'(\xi,\eta)$ the field over the same aperture but optically blocked by obstacles.Let us further assume that it is possible to distribute power blocked by the obstacles over the aperture in the correct direction and phase, and that $F'(\xi,\eta)$ comprises this blocked power. We now want $F'(\xi,\eta)$ and $F(\xi,\eta)$ to be of the same form over the parts of the aperture where $F'(\xi,\eta)$ is defined. Both fields are then related to each other by

$$F'(\xi,\eta) = c.F(\xi,\eta) \tag{45}$$

where c is a constant.

The power P_T radiated by the non-blocked aperture is given by Eq.33. Applying field distribution $F'(\xi,\eta) = c.F(\xi,\eta)$ over the unblocked portion of the aperture A-B, which should radiate P_T as well, leads to

$$P_T = \frac{1}{2}\left(\frac{\varepsilon}{\mu}\right)^{\frac{1}{2}} c^2 \int_{A-B} \left|F(\xi,\eta)\right|^2 d\xi\, d\eta \tag{46}$$

sothat

$$c^2 = \frac{\int_A \left|F(\xi,\eta)\right|^2 d\xi\, d\eta}{\int_A \left|F(\xi,\eta)\right|^2 d\xi\, d\eta - \int_B \left|F(\xi,\eta)\right|^2 d\xi\, d\eta} = \frac{P_T}{P_T - P_B} \quad . \tag{47}$$

or

$$c^2 = \frac{\int_A |F(\xi,\eta)|^2 d\xi\, d\eta}{\int_{A-B} |F(\xi,\eta)|^2 d\xi\, d\eta} \quad . \tag{48}$$

Since the illumination is now multiplied by a factor c , Eq.40b for the new blockage coeficient can now be written

$$\left(\frac{\eta_B}{\eta_0}\right)_{max} = \left| \frac{\int_{A-B} c\, F(\xi,\eta)\, d\xi\, d\eta}{\int_A F(\xi,\eta)\, d\xi\, d\eta} \right|^2 = c^2 \frac{\eta_B}{\eta_0} \tag{49}$$

It will be clear that in the denominator of Eq.49 the field remains unchanged, otherwise the non-blocked aperture would radiate too much power.

Substituting Eq. 48 in Eq. 49 we obtain

$$\left(\frac{\eta_B}{\eta_0}\right)_{max} = \left| \frac{\int_{A-B} F(\xi,\eta)\, d\xi\, d\eta}{\int_A F(\xi,\eta)\, d\xi\, d\eta} \right|^2 \cdot \frac{\int_A |F(\xi,\eta)\, d\xi\, d\eta}{\int_{A-B} |F(\xi,\eta)|^2 d\xi\, d\eta} \quad . \tag{50}$$

Comparison of Eq.48 with Eq.40a shows only a little difference in the denominator. In Eq.50 we find the expression

$$\int_{A-B} |F(\xi,\eta)|^2 d\xi\, d\eta \tag{51}$$

as compared with

$$\int_A |F(\xi,\eta)|^2 d\xi\, d\eta \tag{52}$$

in Eq.40a.

Eq.51 can be explained as being the power radiated by the blocked aperture with the original aperture field $F(\xi,\eta)$. This power is less than that radiated according to Eq. 52.This also means that the blocking efficiency η_B/η_0 will increase as compared with the blocking efficiency presented by Eq.40b.

In case of uniform illumination, $F(\xi,\eta)$ is a constant.

Hence Eq.50 is written as

$$\left(\frac{\eta_B}{\eta_0}\right)_{max} = 1 - \frac{B}{A} \, , \tag{53}$$

which expression was already predicted in Sec. 3 and which also shows that gain and surface are directly proportional to each other, which is normal for antenna systems. This is because no power transmitted by the feed is lost by scattering against the obstacles blocking the aperture.
When looking carefully to the blocked parts of a dual shaped antenna system with blocking obstacles (in the zero field concept), it is easely shown that, if the antenna is used for receiving purposes only, power of the incoming plane waves is intercepted by the obstacles. This power is always wasted and can never be supplied to the feed of a shaped reflector system in the proper way.
We will therefore distinguish between the blocked parts of the aperture, where B_{plane} and B_{sph} represent shadows in the aperture of plane waves and shadows of (nearly) spherical waves, respectively.The optimum blocking efficiency obtainable in the case of uniform illumination, assuming the zero field concept, is therefore

$$\left(\frac{\eta_B}{\eta_0}\right)_{max} = \left| 1 - \frac{\Sigma B_{plane}}{A} \right| \quad . \tag{44}$$

As uniform illumination is assumed, Eq.48 becomes

$$c^2 = \frac{A}{A - B_{plane}} \quad . \tag{48a}$$

5. *Calculations of aperture blockage*

5.1. *Introduction*

The shadows of obstacles within a cassegrain antenna such as subreflector and struts may be treated by geometrical optics, if they are of the same order of magnitude or larger than the wavelength (4,5). Although struts of different constructions are known and applied, this paper will only deal with struts of a cylindrical cross-section, as frequently used in practice. Moreover, not much difference is noticed if rectangular struts are used (1,6).

It has been indicated before (14) that three major areas of shadowing are known (Fig.4a,b and c), assuming no feed blockage.

1. The center obstacle or the subreflector shows a shadow on the aperture obtained byprojecting the subreflector by a plane wave (B_1).
2. The portion of the plane wave obstructed by the struts is found by projecting the struts on the main reflector aperture (B_2) by a plane wave.
3. The third shadow (B_3) is formed by projecting the supports legs on the aperture by a spherical wave with its phase center in the focus (Fig.4b). In the case of shaped systems this shadow is nearly sperical.

The last shadow starts from the point where the supports have been fixed to the main reflector, indicated in Fig.4b by the distance r_o. Owing to mechanical difficulties the supports are very seldom fixed at the rim of a large reflector. Several investigators (1,4,10,14) have made calculations with respect to these shadows more or less approximated. The best possible approximation up till now was first presented by Ruze (1) and his method will now partly be followed here. From the geometry shown in Fig.4, it will be seen that the geometrical surface of the central part B_1 is

$$B_1 = \frac{1}{4}\pi D_s^2$$

and that the geometrical surface of the shadow of the supports is

$$B_2 = 8w(r_o - \tfrac{1}{2}D_s),$$

where it is assumed that the supports are attached to the subreflector, and that four supports will be used. The calculation of the shadow surface from the support legs caused by spherical waves is somewhat more complicated. The projections of the support legs by spherical waves are very similar to trapezoids. Wested (10), however, indicated that the sides of this "trapezoid" are no straight lines, but arcs.

In spite of the small amount of inaccuracy, Wested used the trapezoid approximation. It does, indeed, simplify the calculations and it is to some extent used in this report to discuss the sidelobes caused by blockage. A calculation without approximation is carried out in appendix A. It is found there that for four supports the geometrical surface equals to

$$B_3 = \frac{8w}{AB}\left[\frac{1}{8}D^2 - \frac{1}{2}r_o^2 - \left(\frac{1}{2}D - r_o\right)F\tan\alpha + \frac{\tan\alpha}{12F}\left(\frac{1}{8}D^3 - r_o^3\right)\right] . \qquad (54)$$

5.2. *Uniform illumination*

If the field over the aperture has uniform amplitude and phase distribution, the blockage efficiency $\frac{\eta_B}{\eta_o}$ is readily calculated by

$$\frac{\eta_B}{\eta_o} = \left[1 - \frac{B_1 + B_2 + B_3}{A}\right]^2 = \left[1 - \frac{g_1(o,o) + g_2(o,o) + g_3(o,o)}{g_A(o,o)}\right] , \qquad (55)$$

a being the unblocked geometrical aperture and $\eta_o = 1$. A numerical example has already been discussed in a previous paper (15).
The blockage efficiency has been calculated for uniform field distribution in the aperture as a function of the width of the support legs with the distance r_o as a parameter. Fig. 6a shows the result , being a rapid decrease of efficiency with a growing width of the supports. Moreover, the decrease is less, if the distance r_o is increased, which means that the supports are fixed nearer to the rim of the main reflector. In this case the "trapezoid" shadow decreases and therefore $\frac{\eta_B}{\eta_o}$ improves .

If the width of the supports is neglected in respect of the wavelength, which is possible in some applications, viz. in satellite antennas, the blockage coefficient is entirely depending on the ratio D_s/D. This ratio is mostly 0.1, therefore η_B/η_o is 0.98. Improvement to 0.99 is possible by using special shaping techniques in double reflector systems (9). Trentini (4) has used a different method of calculating the blockage coefficient by introducing an average width of the support. The disadvantage of this method lies in the fact that no clear insight is available as to which part of the shadow is formed by spherical waves and which by plane waves. However, his calculations for uniform distribution are as good as correct. For $D = 350\ \lambda$, $D_s = 35\ \lambda$, $2w = 2\ \lambda$ and $r_o = 90\ \lambda$ his predicted blockage efficiency appears to be 92 %, while the exact calculations shown above indicate a result of 89 % (Fig. 6a).

5.3. *Tapered illumination*

If the illumination of the aperture is tapered towards the edges, the shadows discussed in the previous section will have to be weighted by the aperture illumination function in order to calculate the blockage efficiency. Dealing with such problems, polar coordinates r',ϕ' are mostly used, r' being normalized to unity. Sometimes r is not normalized. The aperture distribution is F(r',ϕ') or F(r,ϕ). Sciambi (16,17) assumes the aperture illumination function to be circularly symmetrical and tapered on a uniform pedestal (Fig. 7). The function may be expressed by

$$F(r') = q + (1-q)(1-r'^2)^p \quad , \quad 0 \leq q \leq 1 \quad , \quad 0 \leq r' \leq 1 \quad . \tag{56}$$

With this illumination function a great variety of aperture distributions may be realized by varying the parameters q and p. The illumination function is also very similar to illuminations obtained by primary feed patterns of scalar feeds and theoretical $2(n+1)\cos^n\psi$ patterns. Uniform illumination is obtained for q = 1, and for q = 0, the aperture is fully tapered. Doidge (18) has used this illumination function to calculate the blockage efficiency for the case of a circularly symmetrical obstacle in the center of the aperture. His final expression contains some inaccuracies and should be

$$\frac{\eta_B}{\eta_0} = \left[1 - \frac{q\Delta^2(p+1) - (1-q)(1-\Delta^2)^{p+1} + 1 - q}{1+qp} \right]^2 \quad . \tag{57}$$

Fig. 8 shows this revised blockage efficiency as a function of the edge illumination, where Δ , being the ratio D_s/D equals 0.1.

Several authors, such as Wested (10), use the aperture illumination function

$$F(r') = 1 - ar'^2 \quad , \quad 0 \leq r' \leq 1 \quad , \quad 0 \leq a \leq \frac{\lambda}{D} \quad , \tag{6}$$

discussed before. Wested has introduced very useful information by calculating the blockage effects caused by plane and spherical waves, although the projection of the supports by spherical waves was approximated by a trapezoid. It appears, however, that the variation in the calculated efficiency is less than 1 per cent when either cylindrical or conical spars with opposite orientations are used (10). Therefore, the shape of the spars seems unimportant with regard to the gain performance, as presumed before.

Gray (19), too, has carried out calculations on the blockage coefficient using an aperture distribution of $1 - r'^2$, $0 \leq r' \leq 1$.

This distribution, however, is not very realistic. In addition, Gray located the struts at the rim of the main reflector, which is seldom done in practice. Moreover, the work contains some inaccuracies as already observed by Wested. Gillitzer (20) should also be mentioned here, although his approach is somewhat different from the others. Following his method, calculations have been carried out of the blockage effect on antenna gain and sidelobes (9).
In the following we will calculate as accurately as possible the blockage effects when the illumination is tapered and we will make use of the results found in the previous sections.
To calculate the tapering effect, in this paper the aperture distribution of Eq. 6 has been used as it is a function resulting in easy mathematics and giving a good insight into the tapering problems (Fig. 2).
The contributions to the blockage efficiency, mentioned in Eq. 55 are now readily found from the theory in Sec. 2. This results in the contribution due to the sub-reflector, viz.:

$$g_1(0,0) = \pi \left(\tfrac{1}{2} D_s\right)^2 \left[1 - \tfrac{1}{2} a \left(\tfrac{1}{2} D_s\right)^2\right] . \tag{12}$$

The contributions to plane-waveblockage by the struts will be

$$g_2(0,0) = 8w\left[r_0 - \tfrac{1}{2} D_s\right] - 8aw\left[\tfrac{1}{3} r_0^3 - \tfrac{1}{3}\left(\tfrac{1}{2} D_s\right)^3\right] - 8aw^3\left(\tfrac{1}{3} r_0 - \tfrac{1}{6} D_s\right) . \tag{17}$$

The contribution to spherical waveblockage by the struts may be found from Eq. 20. However, as this is only an approximation, the contribution by spherical waves discussed in appendix A has been taken for the (0,0) direction resulting in:

$$g_3(0,0) = \frac{8w}{AB}\left[\tfrac{1}{2}\left\{\left(\tfrac{1}{2} D\right)^2 - r_0^2\right\} - F \tan\alpha \left(\tfrac{1}{2} D - r_0\right) + \frac{\tan\alpha}{12F}\left\{\left(\tfrac{1}{2} D\right)^3 - r_0^3\right\}\right] \tag{58}$$

$$- \frac{8wa}{AB}\left[\tfrac{1}{4}\left\{\left(\tfrac{1}{2} D\right)^4 - r_0^4\right\} - F \tan\alpha \cdot \tfrac{1}{3}\left\{\left(\tfrac{1}{2} D\right)^3 - r_0^3\right\} + \frac{\tan\alpha}{4F} \cdot \tfrac{1}{5}\left\{\left(\tfrac{1}{2} D\right)^5 - r_0^5\right\}\right] .$$

Compared with Eq. 20 the difference is only a few per cent.
The final blockage efficiency may now be found from

$$\frac{\eta_B}{\eta_0} = \left[1 - \frac{g_1(0,0) + g_2(0,0) + g_3(0,0)}{g_0(0,0)}\right], \tag{55}$$

$g_1(0,0)$, $g_2(0,0)$ and $g_3(0,0)$ having been discussed in the previous sections. Using Eq. 7, $g_0(0,0)$, being the aperture surface weighted by the aperture illumination function, is found by

$$g_0(0,0) = \int_0^{2\pi} d\varphi \int_0^{\frac{1}{2}D} (1 - ar^2)\, r\, dr \qquad \text{or}$$

$$g_0(0,0) = \pi \left(\tfrac{1}{2}D\right)^2 \left[1 - \tfrac{1}{2}a\left(\tfrac{1}{2}D\right)^2\right], \quad 0 \leq a \leq \frac{2}{D},$$

as discussed in Sec. 2.
The results of a computing program (appendix C) are shown in Fig. 6 b, c and d, where the blockage efficiency has been calculated as a function of the width 2w, r_o and a. $D/D_s = 0.1$.

5.4. *Results and conclusions*

As may be expected, it appears that the blockage efficiency decreases with increasing taper, although for small values of r_o (110-130λ) and for large values of the width of the struts (4-5λ) not much difference is noticed. For a specific value of $r_o = 110\lambda$ ($r_o = \frac{1}{3}D$) and $2w = 2\lambda$ it hardly matters whether the aperture illumination has been tapered towards the edges or not. This phenomenon is due to the fact that the blockage by spherical waves, which is largest, decreases if r_o becomes large. For one particular case, viz. where $D = 330\lambda$, $r_o = 110\lambda$, $D_s = 33\lambda$, and $\psi_2 = 75$ degrees, calculations (app. C) of a uniformly illuminated aperture have been carried out in such a way that the contributions of each obstacle are clearly presented (Fig. 9). We see that the blockage by spherical waves is the most important of all, but also for $2w > 2.25\lambda$ that the plane wave blockage by the struts becomes more significant than that by the subreflector. Although, Eq. 58 contains the parameter F/D ratio of the main reflector and AB and α in that equation depend on the F/D ratio (see appendix A), calculation shows that the influence of the F/D ratio may be neglected. Figs. 10a, b, c show this blockage efficiency as a function of F/D and with edge illuminations of 0 dB, -10 dB and -20 dB. As a typical example, $D = 330\lambda$, $D_3 = 33\lambda$ and $2w = 2\lambda$ have been taken with r_o as parameter.

As will be noticed the graphs are nearly independent of ψ_2. This result is not identical with that published by Ruze (1), where the blockage efficiency increases with increasing F/D ratio. No conclusions may be drawn from Figs. 9 and 10 with regard to the blockage efficiency for $2w < \lambda$, as in that case diffraction effects may not be neglected.
As further results of this work it is worth mentioning that the blockage efficiency as indicated by Doidge (18) has been recalculated and improved. A comparison between approximate formulas of blockage by spherical waves with exact formulas shows only little difference. All in all the work presents closed expressions to calculate the blockage efficiency for nearly all practical applications based on geometrical optics.

6. *References*.

1. Ruze J. :
"Feed support blockage loss in parabolic antennas".
Microwave Journal, pp. 76 - 78, December 1968.

2. Silver S. :
"Microwave antenna theory and design".
Mc Graw-Hill, New York, 1949.

3. Pace J.R.:
"Aperture blockage by a subreflector in a cassegrain antenna system".
Electronics Letters, Vol. 4, p. 500 - 501, 15 November 1968.

4. von Trentini G., Romeiser K.P., and Jatsch E. :
"Dimensionierung und elektrische Eigenschaften der 25 Meter Antenne der Erdfunkstelle Raisting".
Frequenz, 19, nr. 12, pp. 402 - 421, December 1965.

5. Kay. A.F. :
"Electrical design of metal space frame radomes".
IEEE Trans. AP-13, nr. 2, pp. 188 - 202, March 1965.

6. Mei K.K. and van Bladel J. :
"Scattering by perfectly conducting rectangular cylinders".
IEEE Trans. AP-11, nr. 2, pp. 185 - 192, March 1963.

7. Cornbleet S. :
"Radiation patterns of circular aperture with structural shadows".
Proc. IEE, Vol. 117, pp. 1620 - 1626, August 1970.

8. Abramowitz M. and Stegun I.A. :
"Handbook of mathematical functions".
Dover Publications, New York, 1965.

9. Dijk J., and Maanders E.J. :
"Optimising the blocking efficiency in shaped Cassegrain systems".
Electronic Letters, Vol. 4, nr. 18, pp. 372 - 373, September 1968.

10. Wested J.H. :
"Shadow and diffraction effects of spars in a cassegrainian system".
IEE Conference No. 21; Design and Contribution of large steerable aerials. London 6-8 June 1966.

11. Afifi M.S. :
"Scattered radiation from microwave antennas and the design of a paraboloid-plane reflector antenna".
Ph.D. Thesis, Delft University of Technology, Netherlands July 1967.

12. Sheftman F.J. :
"Experimental study of subreflector support structures in a Cassegrain antenna".
M.I.T. Technical Report, nr. 416, 23 September 1966.

13. A.P. Hartsuyker, J.W.M. Baars, S. Drenth and Louise Gelato-Volders.:
"Interferometric measurement at 1415 MHz of the radiation pattern of the paraboloid antenna at Dwingelo Radio Observatory".
To be published in IEEE Transactions on Antenna and Propagation, March 1972.

14. Dijk J., Jeuken M., and Maanders E.J. :
"Blocking and diffraction in Cassegrain antenna systems".
De Ingenieur, Vol. 80, pp. 79 - 91 , 1968.

15. Dijk J., Jeuken M and Maanders E.J. :
"An antenna for a satellite communication groundstation".
TH report 68 - E - 01, Eindhoven University of Technology, Netherlands , March 1968.

16. Sciambi A. :
"Instant antenna patterns".
Microwaves, p. 48-60, June 1966.

17. Sciambi A. :
"The effect of the aperture illumination on the circular aperture antenna pattern characteristics".
Microwave Journal, p. 79-84, August 1965.

18. Doidge E.G.:
"Antenna gain as it applies to satellite communication earth stations".
A seminar on satellite earth station technology,
Washington 16-27 May 1966.

19. Gray C.L.:
"Estimating the effect of feed support member blocking on antenna gain and side lobe level".
Microwave Journal, pp. 88-91, March 1964.

20. Gillitzer E.:
"Die Cassegrain-Parabolantenna und andere Antennen für breitband Richtfunk bei 6 GHz".
Frequenz, 16, No. 11, pp. 459-468, November 1962.

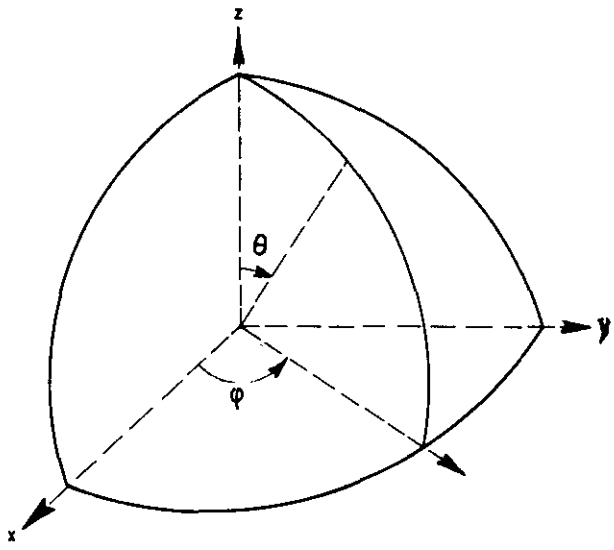

Fig. 1. Spherical coordinates

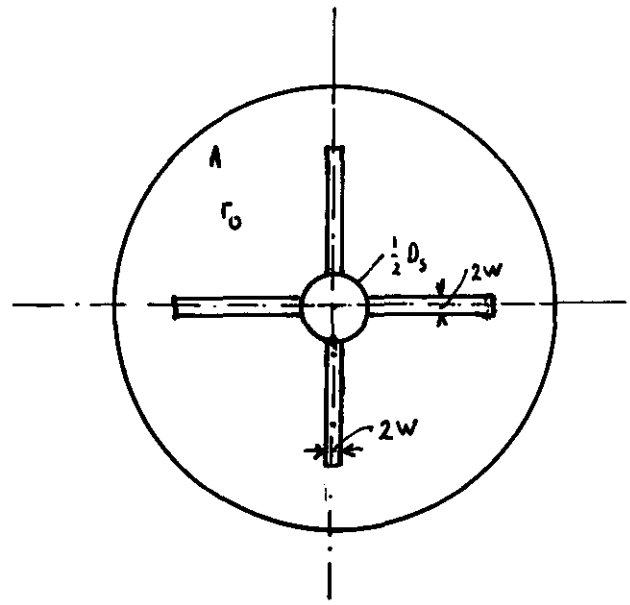

Fig. 3. Blockage by plane waves

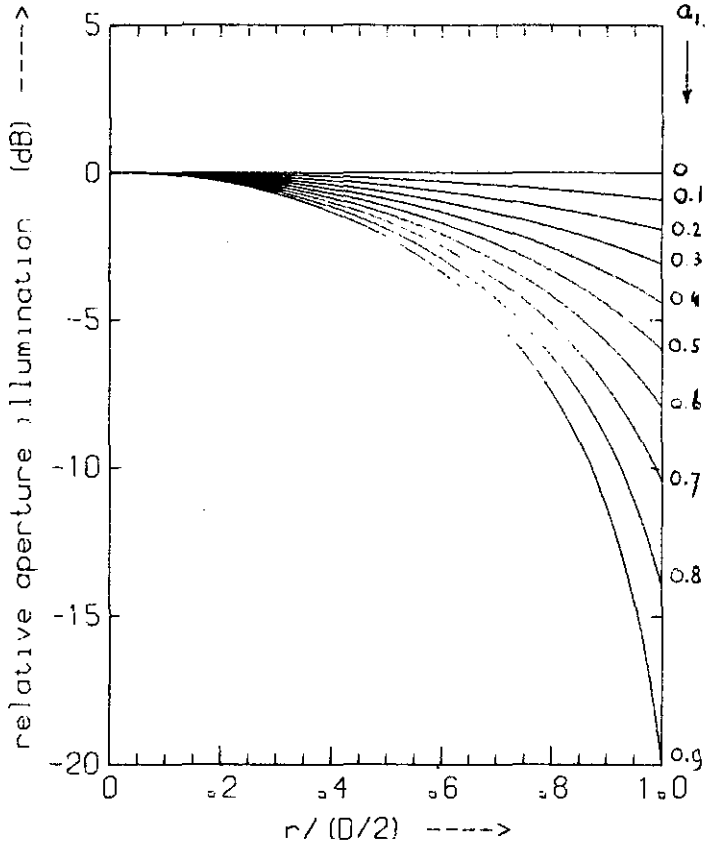

Fig. 2.

Aperture illumination function

$F(r) = 1 - ar_1^2$

$a_1 = (\frac{D}{2})^2 . a$, being

a parameter.

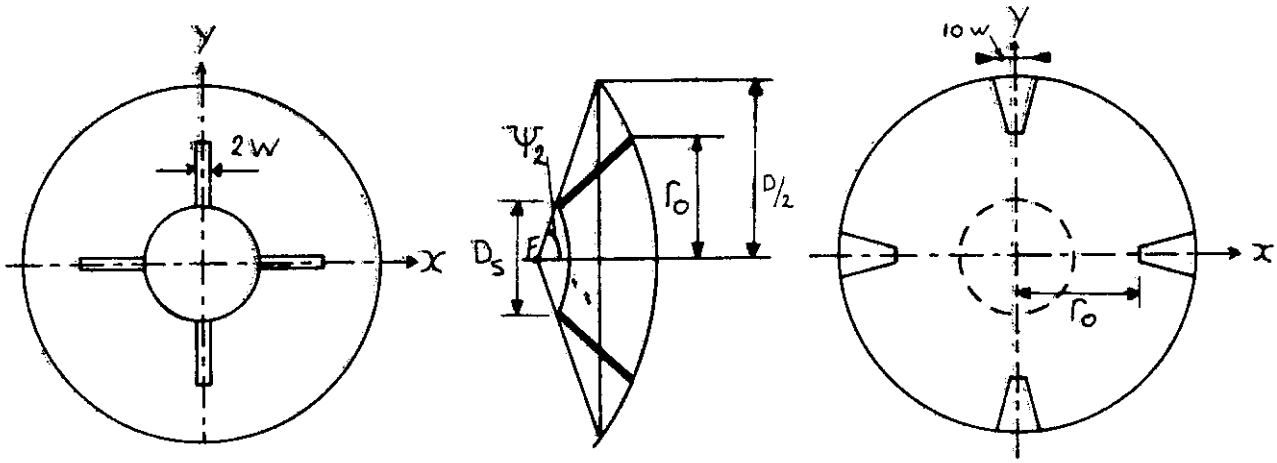

a. b. c.

Fig. 4. Shadowing by plane and spherical waves in cassegrain antenna systems with four struts

a. Shadow by a plane wave

b. Geometry of the antenna

c. Shadow by a spherical wave

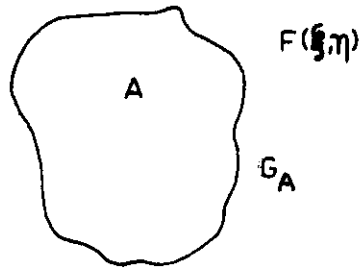

Fig. 5a. Aperture A without blocking

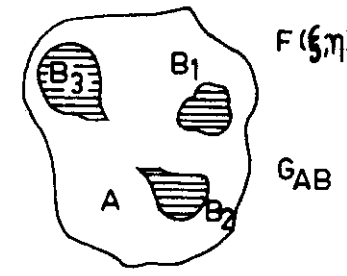

Fig. 5b. Aperture A blocked by obstacles B

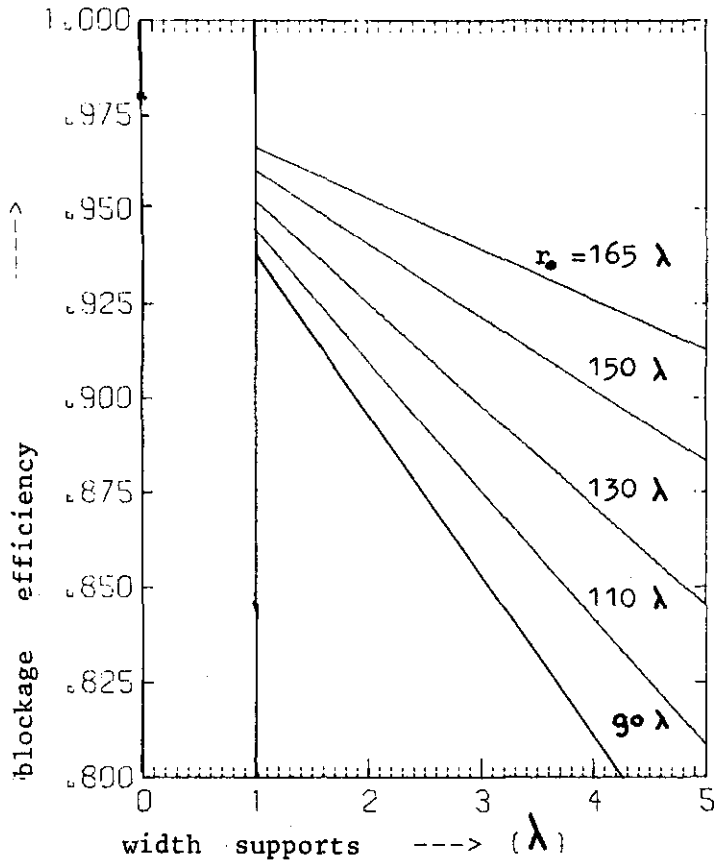

Figure 6a

Blockage efficiency as a function of the width of the supports, r_o being a parameter

$f(r) = 1 - ar^2$

$a = a_1 \cdot (2/D)^2$

$\Psi_i = 75°$
D = 330 λ
Ds = 33 λ
a_1 = 0,0

Uniform illumination

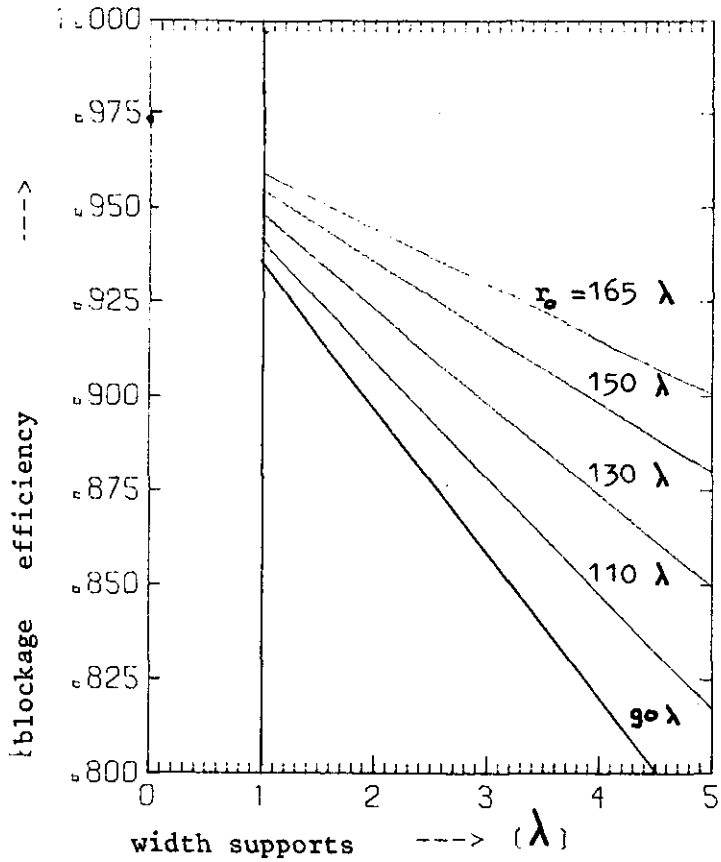

Figure 6b

Blockage efficiency as a function of the width of the supports, r_o being a parameter

$f(r) = 1 - ar^2$

$a = a_1 \cdot (2/D)^2$

$\Psi_i = 75°$
D = 330 λ
Ds = 33 λ
a_1 = 0,5

edge illumination - 6 dB

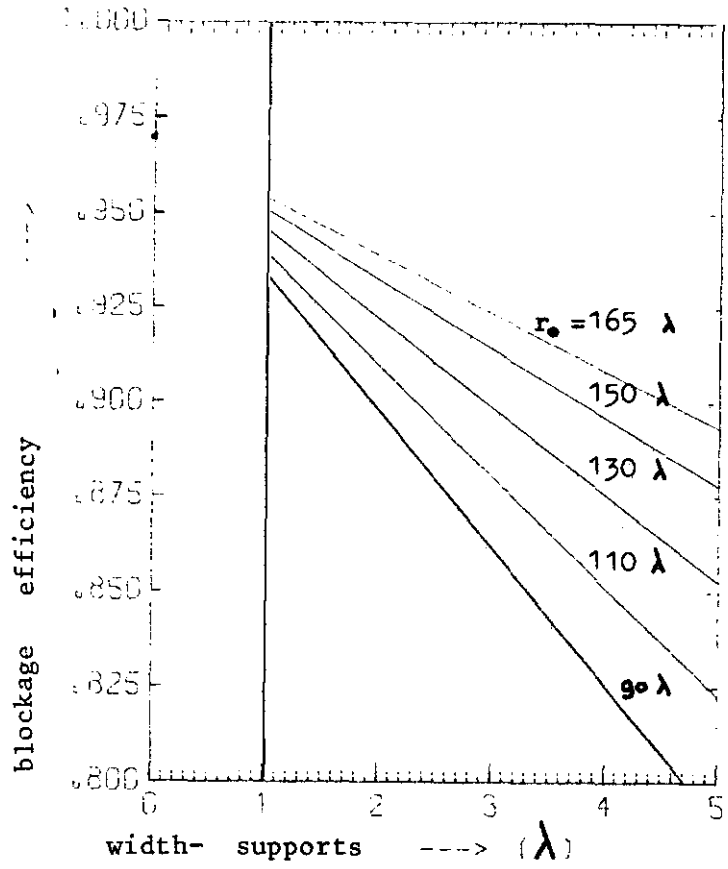

Figure 6c

Blockage efficiency as a function of the width of the supports, r_o being a parameter

$f(r) = 1 - ar^2$

$a = a_1 \cdot (2/D)^2$

$\Psi_1 = 75°$
D = 330 λ
Ds = 33 λ
a_1 = 0,7
edge illumination -10dB

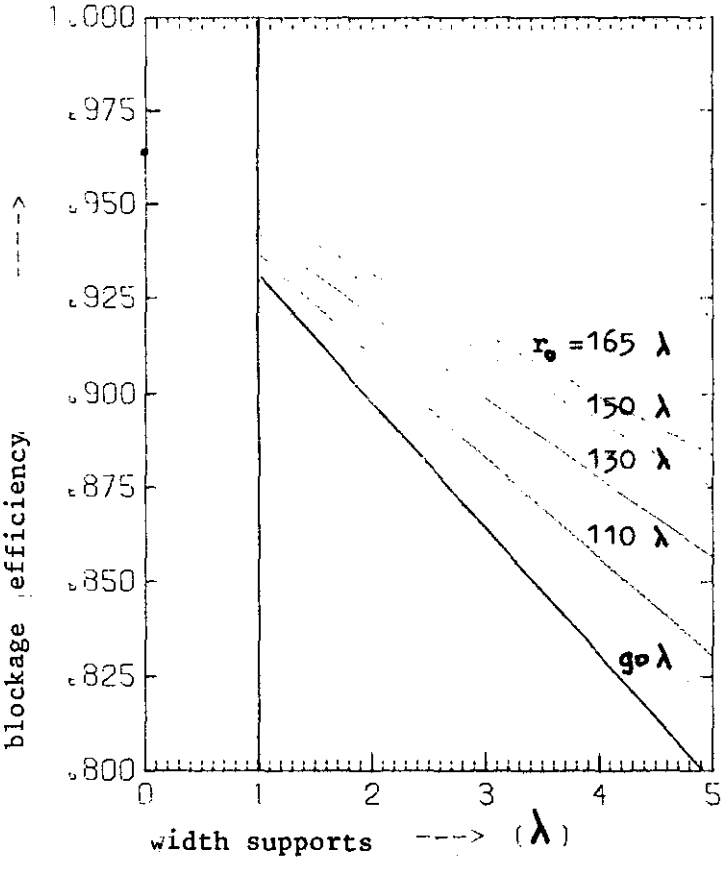

Figure 6d

Blockage efficiency as a function of the width of the supports, r_o being a parameter

$f(r) = 1 - ar^2$

$a = a_1 \cdot (2/D)^2$

$\Psi_1 = 75°$
D = 330 λ
Ds = 33 λ
a_1 = 0,9
edge illumination -20dB

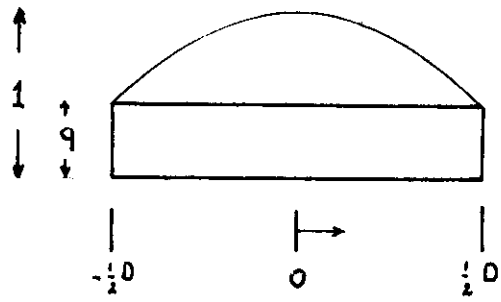

Fig. 7

Aperture illumination function
$F(r') = q + (1-q)(1-r'^2)^p$

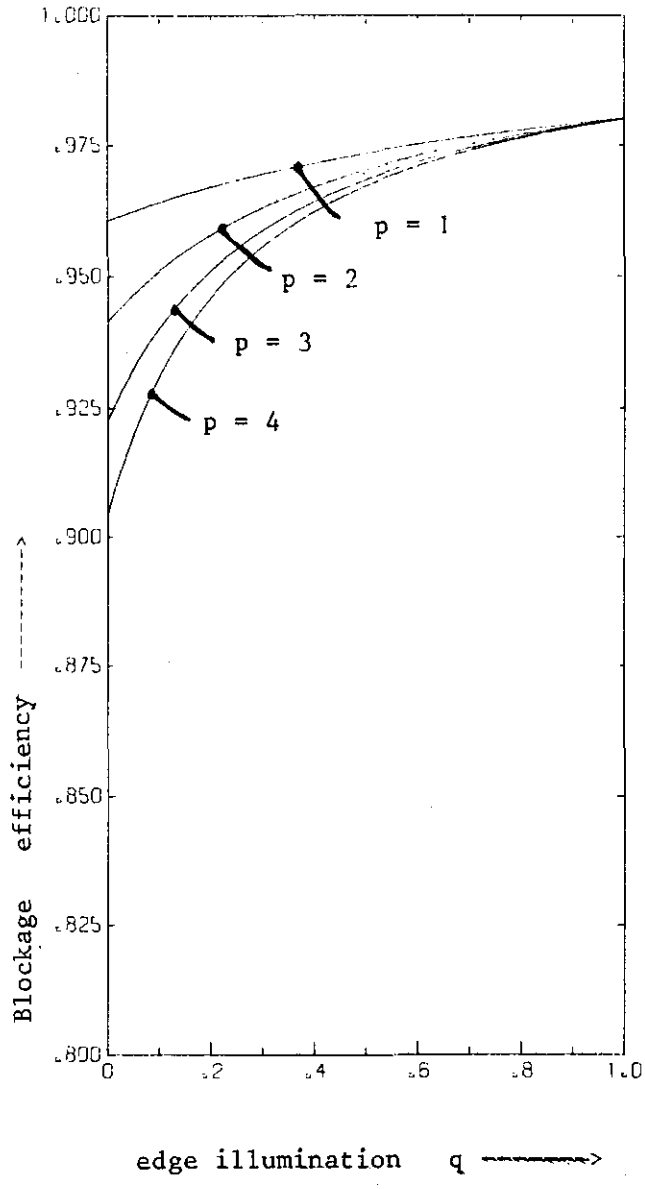

Fig. 8

The blockage efficiency as a function of the edge illumination and p as a parameter using Eq. 54

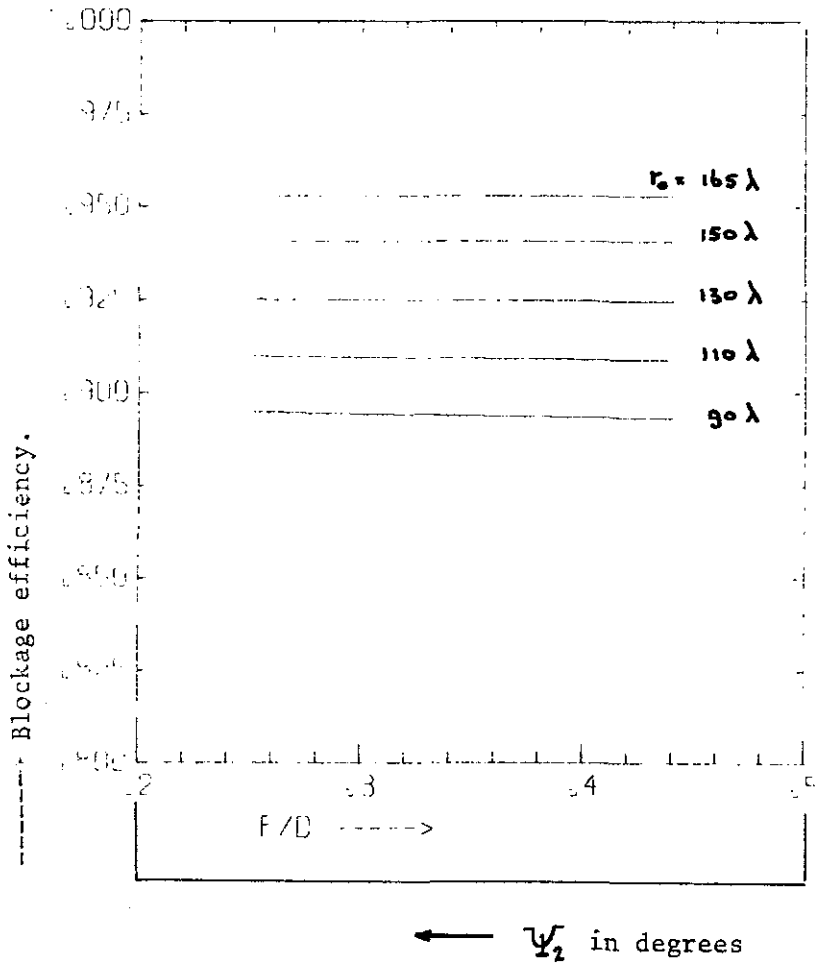

Fig. 10a

Dependence of the blockage efficiency on the F/D ratio of the main reflector.
Uniform illumination.
$D_s/D = 0.1$
$2w = 2\lambda$
$D = 330\lambda$

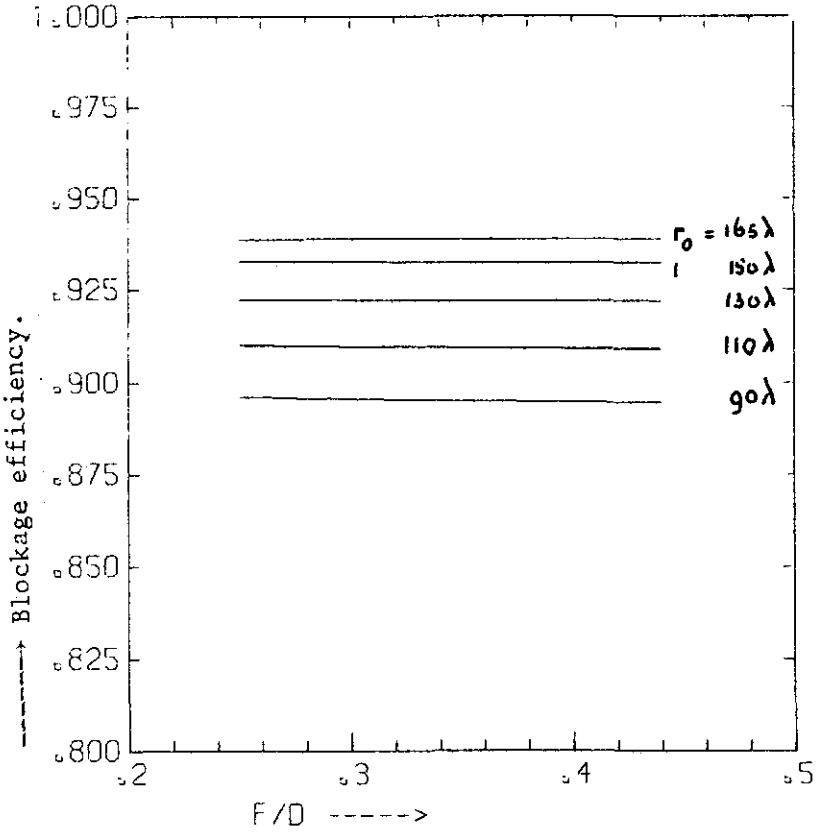

Fig. 10b

Dependence of the blockage efficiency on the F/D ratio of the main reflector.
- 10dB edge illumination.
$D_s/D = 0.1$
$2w = 2\lambda$
$D = 330\lambda$

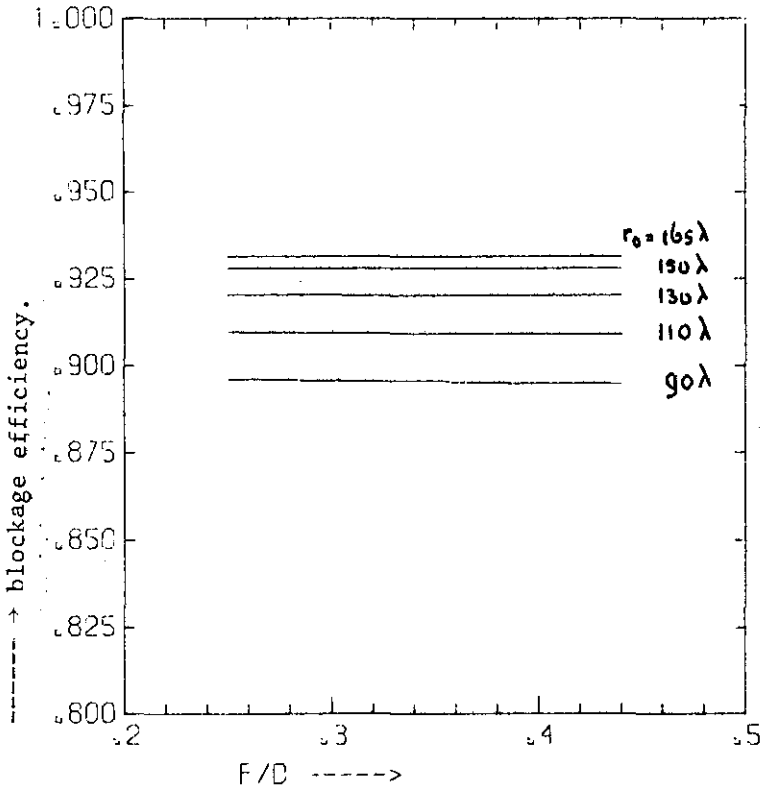

Fig. 10c

Dependence of the blockage efficiency on the F/D ratio of the main reflector.
- 20 dB edge illumination.
D_s/D = 0.1
2w = 2λ
D = 330λ

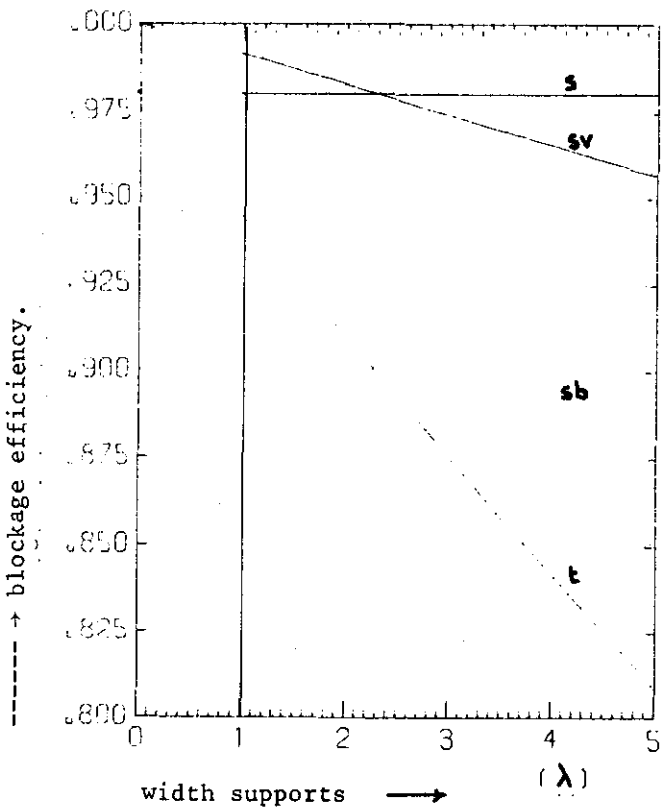

Fig. 9

Contribution of the blocking obstacles to the total blockage efficiency.
s = blockage efficiency of subreflector
sv = blockage efficiency of supports (plane waves)
sb = blockage efficiency of supports (spherical waves)
t = total blockage efficiency
D = 330λ
D_s = 33λ
r_o = 110λ
Ψ_2 = 75°
a_1 = 0 (uniform illumination)

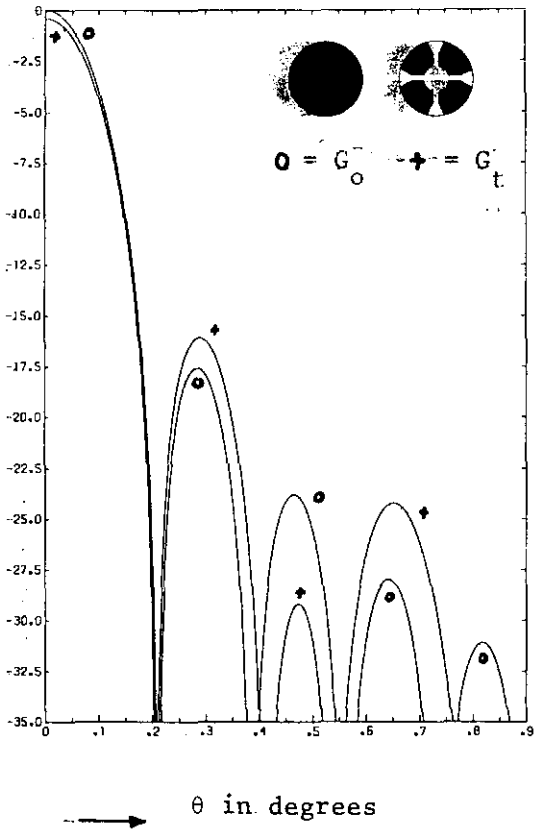

Fig. 11a

Directive gain pattern relative to directivity, uniform illumination

$\varphi = 0$ $\quad D = 330\ \lambda$

$D_s = 33\ \lambda$

$r_o = .110\ \lambda$

$2w = 2\ \lambda$

$$G_o = 10 \log \left| \frac{g_o(\theta)}{g_o(0)} \right|^2$$

$$G_t = 10 \log \left| \frac{g_t(\theta)}{g_o(0)} \right|^2$$

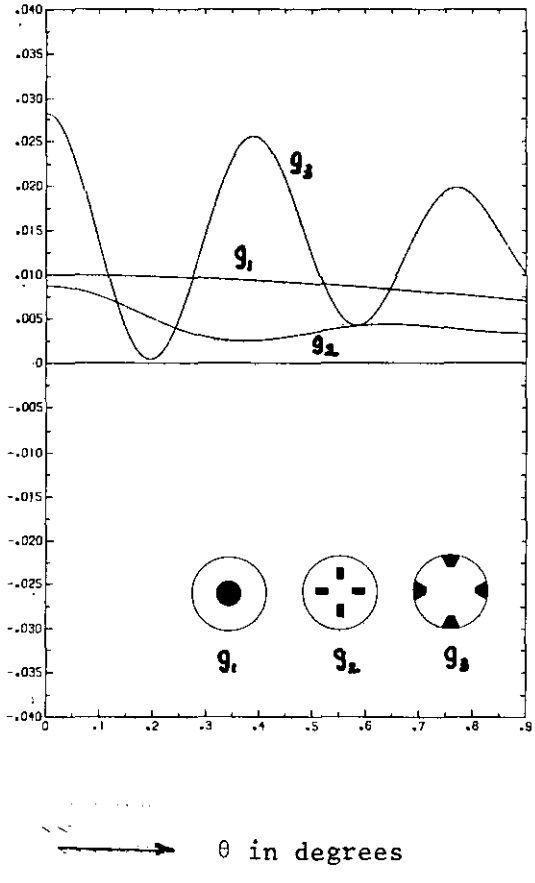

Fig. 11b

Relative patterns g_1, g_2 and g_3, uniform illumination

$\varphi = 0$ $\quad D = 330\ \lambda$

$D_s = 33\ \lambda$

$r_o = 110\ \lambda$

$2w = 2\ \lambda$

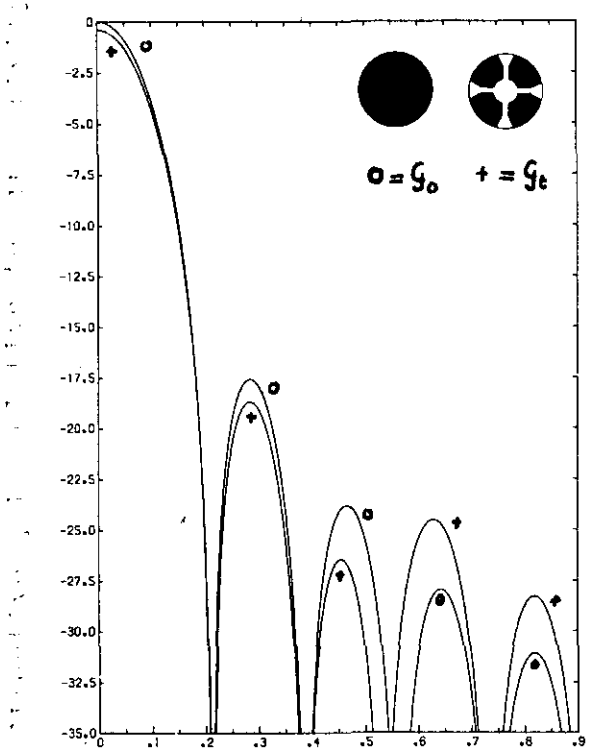

Fig. 12a

Directive gain pattern relative to directivity, uniform illumination.

$\varphi = 45^\circ$ $\quad D = 330\ \lambda$

$D_s = 33\ \lambda$

$r_o = 110\ \lambda$

$2w = 2\ \lambda$

$$G_o = 10 \log \left| \frac{g_o(\theta)}{g_o(0)} \right|^2$$

$$G_t = 10 \log \left| \frac{g_t(\theta)}{g_o(0)} \right|^2$$

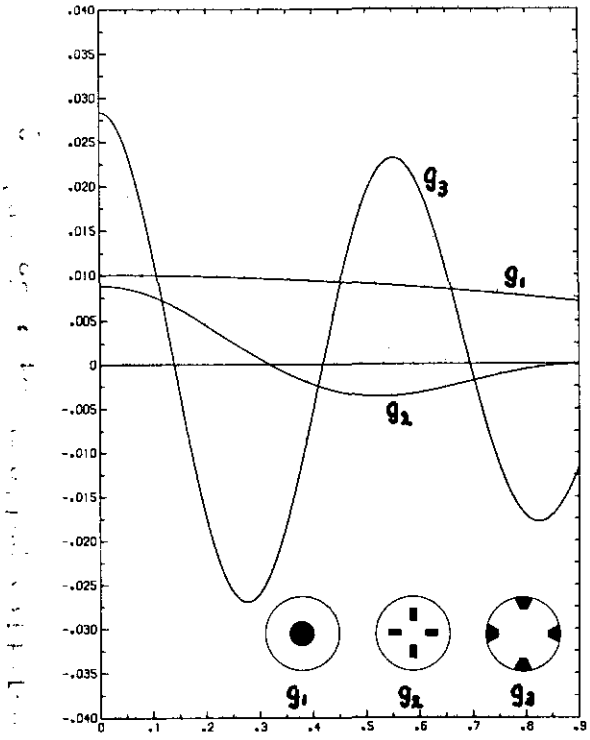

Fig. 12b

Relative patterns g_1, g_2 and g_3.

$\varphi = 0$ $\quad D = 330\ \lambda$

$D_s = 33\ \lambda$

$r_o = 110\ \lambda$

$2w = 2\ \lambda$

Appendix A. Blockage by spherical waves

The geometry required to calculate the "weighted" blockage of the struts caused by spherical waves is found in Fig A_1. Using the law of sines in ABC of this figure we find

$$\frac{AC}{\sin(\alpha+\frac{\pi}{2})} = \frac{AB}{\sin(\psi-\alpha)} \qquad (A1)$$

Further,

$$x' = AC \sin\psi = \frac{AB \cos\alpha \sin\psi}{\sin(\psi-\alpha)}$$

Using in addition Fig. A2, the geometry also shows that

$$\frac{x'}{r} = \frac{AC}{AC'} = \frac{w}{y} \text{ ; therefore}$$

$$y = \frac{wr}{x'} = \frac{wr\sin(\psi-\alpha)}{AB\cos\alpha\sin\psi}$$

As in a cassegrain system (Fig A3) $r = 2F \tan\frac{1}{2}\psi_2$

we find that

$$y = \frac{w}{AB}\cdot\frac{\tan\alpha}{4F} r^2 + \frac{wr}{AB} - \frac{wF}{AB}\tan\alpha \qquad (A2)$$

Therefore,

$$g_3(0,0) = 4\int_{r_0}^{\frac{1}{2}D} (1-ar^2)\, 2y\, dr$$

which results in

$$g_3(0,0) = \frac{8w}{AB}\left[\frac{1}{2}\left\{\left(\tfrac{1}{2}D\right)^2 - r_0^2\right\} - F\tan\alpha\left\{\tfrac{1}{2}D - r_0\right\} + \frac{\tan\alpha}{12F}\left\{\left(\tfrac{1}{2}D\right)^3 - r_0^3\right\}\right] +$$

$$- \frac{8wa}{AB}\left[\frac{1}{4}\left\{\left(\tfrac{1}{2}D\right)^4 - r_0^4\right\} - F\tan\alpha\cdot\frac{1}{3}\left\{\left(\tfrac{1}{2}D\right)^3 - r_0^3\right\} + \frac{\tan\alpha}{4F}\cdot\frac{1}{5}\left\{\left(\tfrac{1}{2}D\right)^5 - r_0^5\right\}\right] \qquad (A_3)$$

For uniform illumination $Q = 0$ Eq. A3 reduces to

$$g_3(0,0) = \frac{8W}{AB}\left[\frac{1}{8}D^2 - \frac{1}{2}r_0^2 - \left(\frac{1}{2}D - r_0\right)F\tan\alpha + \frac{\tan\alpha}{12F}\left(\frac{1}{8}D^3 - r_0^3\right)\right] \tag{A4}$$

The system constants α and AB may be found from Fig. A1 resulting in

$$\tan\alpha = \frac{r_0 - \frac{1}{2}D_s}{2F\,\frac{\cos\Psi_0}{1+\cos\Psi_0} - \frac{\frac{1}{2}D_s}{\tan\Psi_2}}, \tag{A5}$$

and as

$$\tan\alpha = \frac{r_0 - AB}{AB'} = \frac{r_0 - AB}{r_0}\tan\Psi_0,$$

$$AB = r_0\left[1 - \frac{\tan\alpha}{\tan\Psi_0}\right] \tag{A6}$$

and $r_0 = 2F\tan\frac{1}{2}\Psi_0$.

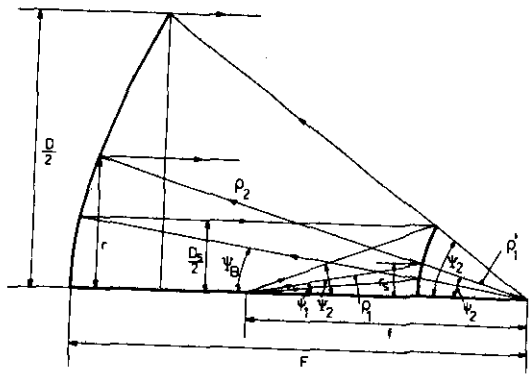

Fig. A_3. Classical Cassegrain system

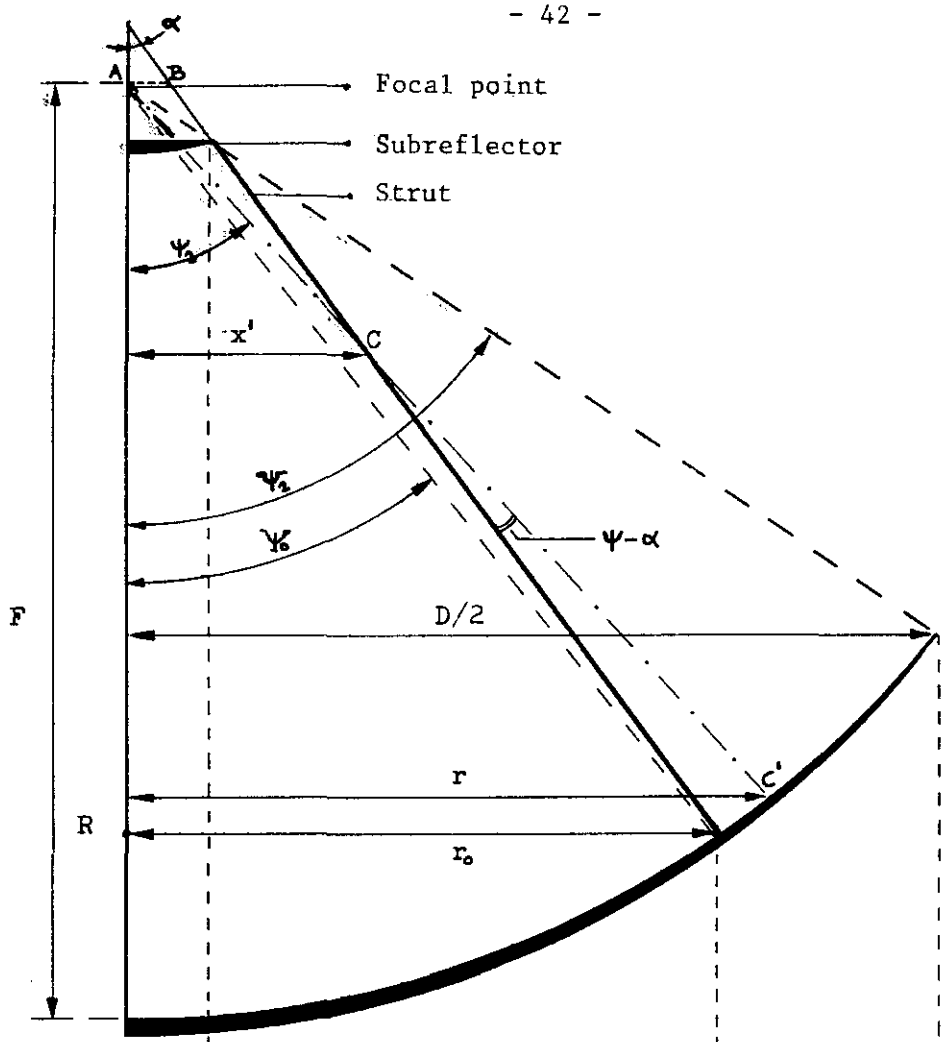

Fig. A_1

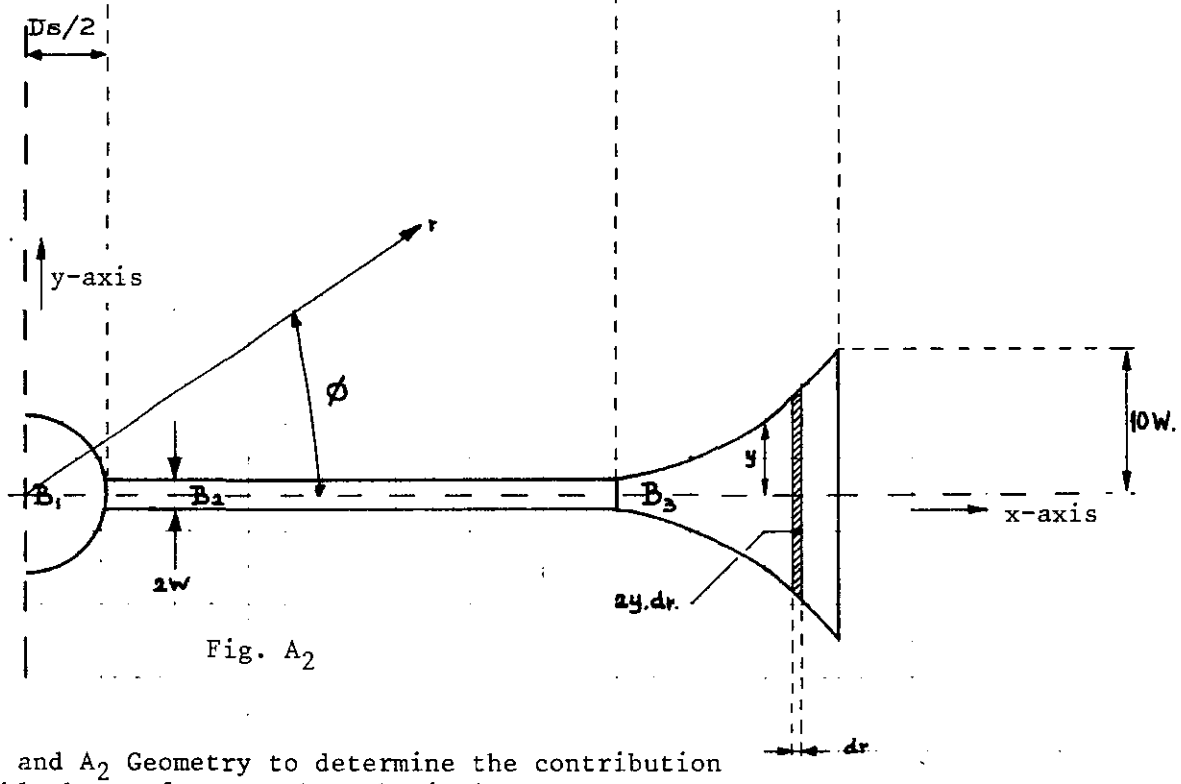

Fig. A_2

Fig. A_1 and A_2 Geometry to determine the contribution to the blockage of struts by spherical waves in cassegrain systems

$$\left(\frac{D_s}{D} = \frac{1}{10} \right)$$

Appendix B

Computer program for the total directive gain pattern $g_t(\theta, \phi)$

Purpose : This program computes the total directive gain pattern near the main axis of a double reflector antenna system blocked by subreflector and subreflector supports.

Language: Algol

Author : J.M.Berends, Eindhoven University of Technology,Dept. of Electrical Engineering, Eindhoven, Netherlands.

Description :

The directive gain pattern may be represented by the expression

$$g_t(\theta,\phi) = g_o(\theta,\phi) - g_1(\theta) - g_2(u,v) - g_3(u,v)$$

where $g_o(\theta,\phi)$ represents the pattern of an unblocked aperture given by Eq.8; $g_1(\theta)$ the contribution to the pattern by the subreflector (Eq.11); $g_2(u,v)$ the contribution due to plane wave shadows (Eq.17); and $g_3(u,v)$ the contribution due to spherical waves (Eq.20).

The variables u and v are represented by $u = \sin\theta.\sin\phi$ and $v = \sin\theta.\cos\phi$

For $\phi = 0$ a value of 10^{-3} has been taken to avoid discontinueties with $\phi = 0$ in the denominator.

Input variables

Input variables on a special input tape are the following : a (Eq.6); wavelength λ; diameter main reflector D in λ ; diameter subreflector D_s in λ ; width of the supports 2w (in λ); r being $D_s/2 \leqslant r \leqslant D/2$; further, Y_{max}, Y_{min} y_{max}, and y_{min} being values determining the vertical coordinates.

Output

The output consists of printed output and plots. There is printed output which prints G_o and G_t in dB, and printed output which prints g_o, g_1, g_2, and g_t, not in dB, both for $\phi = 0$ and $\phi = 45^o$.

The program supplies 6 plots, viz. G_o and G_t in dB, g_o and g_t not in dB but in absolute values, and g_1, g_2, and g_3 both for $\phi = 0$ and $\phi = 45^o$.

Appendix C

Computer program to calculate aperture blockage

Purpose

This program calculates the blockage efficiency as a function of the width of the supports , the edge illumination of the main reflector, the implantation of the supports on the main reflector and the F/D ratio of the main reflector.

Language : Algol

Author : J.M.Berends, Eindhoven University of Technology,
Department of Electrical Engineering, Eindhoven, Netherlands.

Description

The blockage efficiency has been calculated by means of the formula

$$\frac{\eta_B}{\eta_o} = \left[1 - \frac{g_1(0,0) + g_2(0,0) + g_3(0,0)}{g_0(0,0)}\right]^2$$

where $g_1(0,0)$ is represented by Eq. 12 ,$g_2(0,0)$ by Eq.17 ,$g_3(0,0)$ by Eq. 20 and $g_o(0,0)$ by Eq.10.

Input variables

Before starting the program the following parameters have to be fixed: D in λ, Ψ_2 in degrees, D_s in λ. From D and Ψ_2 the focal distance F may be calculated. Four values of a ,determining the edge illumination should read in>duced as well as four values fo r_o (the implantation of the struts on the main reflector)

Output

The output consists of printed output and plots. The printed output gives the efficiency as a function of 2w, which varies between 0 and 5λ . The implantation (r_o) is parameter. For D = 330 λ, a suitable value for satellite communication, r_o varies between 90 λ and 165 λ.It is also possible to obtain the blockage efficiency as a function of F/D with r_o again being parameter and variable edge illumination.

The plots supplied with this program show the blockage efficiency as a function of the edge illumination with varying support width and r_o as parameter or as a function of F/D with constant support width and varying edge illumination.